Master's thesis

NTNU
Norwegian University of Science and Technology
Faculty of Natural Sciences
Department of Geoscience and Petroleum

Regine Hagen

Understanding Coastal Processes and Evolution by Geomorphological Mapping along the North-Eastern Coastline of Prins Karls Forland, Svalbard

Master's thesis in Geology
Supervisor: Maarten Felix
Co-supervisor: Maria Jensen
May 2022

Regine Hagen

NTNU
Kunnskap for en bedre verden

Regine Hagen

Understanding Coastal Processes and Evolution by Geomorphological Mapping along the North-Eastern Coastline of Prins Karls Forland, Svalbard

Master's thesis in Geology
Supervisor: Maarten Felix
Co-supervisor: Maria Jensen
May 2022

Norwegian University of Science and Technology
Faculty of Natural Sciences
Department of Geoscience and Petroleum

NTNU
Norwegian University of
Science and Technology

ABSTRACT

During the last 100 years a rise in temperature, especially during winter, has been observed in the Arctic. As a result, glaciers retreat, the active layer of permafrost increases in depth, the open water season becomes longer, and storms become stronger and more frequent. All these changes affect and will continue to affect Arctic coastlines. To improve the understanding of Arctic coastline changes of Prins Karls Forland, Svalbard, field observations and the study of aerial photos and satellite images from 1936, 2008 and 2021 were combined to map the geomorphological and sedimentological features and changes. Fieldwork was carried out at 8 localities on the north-eastern shore of Prins Karls Forland during the summer of 2021. Grain size data, landform descriptions, vegetation cover descriptions and samples for 14C dating were collected during the fieldwork. At each locality, landforms (as seen in the field) and their changes (as seen from satellite images) were used to identify the processes controlling shoreline morphology (wave action, tides, coastal currents, …). The combined fieldwork/ image analysis showed that the main process controlling shoreline morphology is wave action due to incoming swells/ waves from the north. The main process is however overprinted at Selvågen and Brebukta by tidal influence and terrestrial processes in sheltered bays and recently deglaciated areas. The future development of the north-eastern coastline of PKF is predicted on the basis of current processes observed and climatic trends. Coastal sections that are sheltered from strong swells/ waves will likely prograde as terrestrial processes and paraglacial sedimentation provide sediment, while coastal features found along wave exposed coasts will likely migrate landwards due to increased storminess.

SAMMENDRAG

Feltarbeid på Prins Karls Forland fant sted i september 2021. Ulike prosesser som bidrar til utviklingen av kystlinja ble kartlagt, beskrivelser av sedimenter som utgjør strandsonen ble gjort og prøver tatt med til C-14 dateringer. Observasjonene gjort i felt dannet sammen med flyfoto og satellitt-bilder fra Norsk Polarinstitutt grunnlaget for de geomorfologiske og overflate-sedimentologiske kartene presentert i denne master-oppgaven. Flyfoto og satellitt-bilder fra NPI har også bidratt forståelsen av landskapets kystutvikling. Kystlinje-utviklingen langs den nord-østlige delen av Prins Karls Forland er hovedsakelig bølgedominert, men lokale prosesser dominerer hvor bølgene ikke strekker til. Informasjonen innhentet fra Prins Karls Forland er overførbar til andre deler av Arktis hvor folk og infrastruktur rammes av kystendringer.

ACKNOWLEDGEMENTS

Many people deserve a huge THANK YOU:

- Maria Jensen at UNIS for giving me this opportunity. Exploring the coast of Prins Karls Forland has been interesting, challenging, rewarding and given me a once in a lifetime experience.
- Ronja Arum for wanting to be my field assistant and managing to attend the fieldwork in such a short notice. It was great to get to know you at the very remote island far away in the Arctic. Thank you for keeping the mood in the afternoons when I was cold and not motivated.
- Maarten Felix for direct and precise feedback. You always have the time, you are always in a good mood, and I have appreciated having you as a supervisor.
- Gareth, Øyvind, Ragnar and Ola for reading through and being supportive.
- Hr Ulv for giving me good breaks and time outside, no matter weather. And Anne and Ola, for walking the dog when I was at Svalbard. I know you support me.
- Tor Geir for support, good conversations and always being there for me.

TABLE OF CONTENTS

FIGURES

TABLES

ABBREVIATIONS

PKF	Prins Karls Forland
NPI	Norwegian Polar Institute
MHT	Mean High Tide
MLT	Mean Low Tide

LOCATION NAMES

Original place names have been used in this study. Many of these ascribe the nature or landform by having a descriptive suffix. The names of the study sites have the suffixes listed below and the translation to English is given in the column to the right.

Breen/ breene	The glacier/ the glaciers
Bukta	The bay
Fjellet	The mountain
Flya	The lowlands
Isen	The glacier ice
Laguna	The lagoon
Neset	The headland
Pynten	The headland
Stranda	The beach
Sundet	The sound
Tangen	The headland
Tjørn/ tjørnene	The lake/ the lakes
Vågen	The bay

1 INTRODUCTION

Arctic permafrost coasts constitute 34 % of the world's coastlines (Lantuit et al., 2012). The coastline around the Svalbard archipelago is 8782 km long, of which only 8.7% has been geomorphologically mapped (Lantuit et al., 2012). Arctic coastlines are under the influence of permafrost and/ or seasonal ice cover which give rise to unique landforms and processes. Furthermore, these coastlines are prone to rapid and extensive alteration as climate changes its character. The present warming of the climate is occurring at a greater rate in the Arctic regions than in temperate areas (Kattsov et al., 2005). This influences coastal development by altering several factors that are intrinsically linked to coastline development such as water-surface temperature and weather, including wind and precipitation. On any coastline, storm generated waves can displace great amounts of sediment which may lead to considerable changes of the coastline morphology. As permafrost regions thaw, the ground loses its competence and erosion caused by waves can occur more readily, thus coastlines that have typically been considered stable become more exposed to the same processes that affect their warmer climate counterparts.

In regions of the Arctic where archaeological sites are present, people are habituated or infrastructure exposed to coastal changes, the coastline requires close attention, especially with regards to the monitoring and protection of historic sites, roads, infrastructure, and homes, as well as prevention of incidents that may cause loss of life. Therefore, a greater knowledge of the different processes, the evolution and the vulnerability of Arctic coasts is fundamental in establishing appropriate tools for protection and adequate adaptation practices.

This thesis provides geological data regarding the north-eastern coastline of Prins Karls Forland, (PKF), an 89 km long island of 615 km^2 (toposvalbard.npolar.no) located on the western margin of Spitsbergen (Figure 1A & B). The study sites span over 50 km from Heemskerckneset in the north to Dawespynten in the south. Until this present study, no coastal evolution studies have been conducted on Prins Karls Forland. The information gathered in this thesis will be used to project future coastal development considering recent climate change and thus contribute to the understanding of Arctic coasts in a warming climate.

Figure 1 Location of interest. A: Location of Svalbard. B: Overview of Prins Karls Forland on Svalbard. Green box shows location of the study area. C: Study area in more detail. Each study site is labelled. White boxes: mapped coastal morphology. Background map and satellite image courtesy of NPI. Legend to all maps provided by NPI can be found in the appendix.

Fieldwork took place in September 2021 when the different processes that control the coastal evolution were observed, samples gathered from logs and a whale bone from different landforms were collected for C-14 dating and sediments that compose the shoreline at Andeneset, Sessflya and Selvågen were described. The processes observed along with aerial photos provided by NPI formed the bases for making geomorphological and surficial sedimentological maps. The dominating process and local influencing processes that control coastal evolution has been recognize. Propositions for former evolution are given on the basis on geomorphological features observed.

1.1 Main Objectives

The objectives for the current study were:

1. To map geomorphological features based on field observations and aerial photographs.
2. To gain perspective on differences in coastal development between sections of the coastline that were unglaciated 85 years ago and sections that were covered with glacier ice in 1936 by studying legacy aerial photos and modern satellite images provided by the Norwegian Polar Institute (NPI).
3. Identify dominant hydrodynamic processes acting on the coastline in the study area.
4. Use surficial geomorphological features to deduce barrier evolution, record changes over the last 85 years by studying aerial photos provided by NPI and correlate the findings to already existing models of barrier development.
5. To estimate future development of the coastline.

These objectives were addressed by trying to answer the following specific questions:

1. What are the key physical processes that dominate and/ or influence the coastal evolution of north-eastern Prins Karls Forland?
2. Which factors control coastal development in recently deglaciated vs non-glaciated regions?
3. How can the coastal processes observed in the study area be used to predict future coastal development?

2 BACKGROUND THEORY

The next pages give a brief theoretical overview of information regarding Carbon 14 analysis, grain sizes, Arctic conditions, processes, and landforms.

2.1 General Background

As this study focuses on geomorphological elements and processes that influence and dominate the coastline, the unconsolidated sediments are in focus. All consolidated geology is defined as bedrock in this thesis.

2.1.1 Carbon 14 Analysis

Dating organic material can be performed on samples younger than 50 000 years by comparing the amount of Carbon 14 to the ration between atmospheric Carbon 14 and Carbon 12. Material from several geological archives such as ice cores, marine sediment cores, terrestrial sequences and remains from living creatures can be dated. The volume of a sample and its age impact the accuracy of carbon dating; e.g. the smaller and older, the greater the decay and/or pollution of modern atmospheric carbon might be (Gottschalk et al., 2018). This causes uncertainty regarding intrinsic age of the sample.

2.1.2 Sediment Grain Size

To determine siliciclastic sediment grain sizes in the field, a grain size chart (after Udden, 1914) and a 10x magnification hand lens (loupe) were used as a foundation for contemporary field observations. Nomenclature and grain sizes observed in the field correspond to those defined in Table 1.

Table 1 Nomenclature for grain sizes. After Udden (1914).

Particle size [mm]	Classification	Fraction	
		Unlithified	Lithified
< 0.004	Clay	Clay	Mudstone
0.004 - 0.063	Silt	Silt	or Shale
0.063 – 0.125	Very fine sand	Sand	Sandstone
0.125 – 0.25	Fine sand		
0.25 – 0.5	Medium sand		
0.5 – 1	Coarse sand		
1 - 2	Very coarse sand		
2 - 4	Granule	Gravel	Conglomerate
4 – 64	Pebble		
64 - 256	Cobble		
256 - 4096	Boulder		

2.2 The Coastal Area

Definitions of the specific terms used in this thesis are from the chapter Shorelines by (Lutgens et al., 2014a). The *coastline* is the seaward boundary of the coast. The *coast´s* inland boundary is where sea-related features no longer can be found. This boundary can often be difficult to establish. The *shoreline* is the boundary between land and sea and the *shore* is the section "between the lowest low tide and highest elevation point on land that is affected by storm waves". The *foreshore* is the area between low and high tide. The *backshore* is the "area landward of the high-tide shoreline and is only affected by waves during storms".

2.3 Arctic Conditions

Coastal dynamics in an Arctic environment depends on heavily on the state of ground: the presence or absence of permafrost, lithified or unlithified material exposed at the coast as well as the prevailing local weather and hydrological conditions. A previously glaciated landscape that becomes deglaciated can be denoted as a paraglacial landscape which is defined by Church and Ryder (1972) as a landscape dominated by "nonglacial processes that are directly conditioned by glaciation". The term *paraglacial* incorporates a variety of processes; glacial, periglacial, proglacial and slope processes all of which can interfere and influence coastal development. According to French (2000) a *periglacial* environment should be considered to be the same as a "cold, non-glacial environment". Periglacial environments are characterized by the presence of permafrost and are strongly influenced by frost-processes. A *proglacial* environment is defined at the margin of a glacier or an ice sheet (French, 2000).

Both thermal and mechanical influence must be considered when studying coastal evolution in the Arctic. Islam et al. (2020) identified two significant erosion mechanisms: thermal denudation and thermal abrasion. *Thermal denudation* is the response of ice content (permafrost) within sediment situated on thawing ground and slopes to air temperature and solar radiation, which consequently results in downwards transportation of sediments by gravity (Shur & Osterkamp, 2007). *Thermal abrasion* is an erosive process involving both thermal and mechanical energy from the sea (Are, 1988).

2.3.1 Sea Ice

The sea ice extent in the Arctic has a maximum extent in March and a minimum in September. Over the last 50 years, the sea ice extent in Arctic regions has decreased markedly. September is the month that has experienced the greatest loss with 8.6% per decade while March only had a 2.8% decrease per decade (Serreze et al., 2007). Sea ice extent influences climate on a global level as reduction of sea ice will lead to decreased reflection of solar radiation, and alterations in sea ice extent can influence atmospheric circulation via changes in surface fluxes and moisture (Bader et al., 2011). On a local level, sea ice has a direct impact on the strength of storms (Simmonds & Keay, 2009).

The greatest effect of sea ice is protective, but it must be emphasized that sea ice can erode as ice is being pushed onshore by winds and hence scour the shoreline (Forbes & Taylor, 1994a).

2.3.2 Permafrost

The scope of permafrost along with wave exposure are the two foremost factors that influence character and rate of coastal changes (Irrgang et al., 2022). Permafrost is a physical state of the ground defined as permanent freezing of the ground with ground temperatures that do not exceed 0°C for at least two consecutive years (Harris et al., 1988b). Permafrost ground consists of sediment and ice within the ground. There are several factors that influence permafrost such as solar radiation, energy transfer between ground surface and atmosphere, topography, snow cover, lithology, and geothermal heat flow. The most important factors are however climate and distance to the ocean (Sollid & Christiansen, 2003). Air temperature, wind, and snow cover are factors controlled by climate. Kristensen et al. (2008) modelled sea water to impact ground temperature at depth 100 m inland. Ground temperatures near the surface were found to be controlled locally (Kristensen et al., 2008) by factors listed above. In central parts of Spitsbergen, permafrost depth is 450 metres (Liestøl, 1977) while at the coast, depth is only 100 metres or less (Humlum et al., 2003).

The top layer of the permafrost which thaws during summer is called the active layer. The layer is influenced by changes in summer temperatures. At coastal sites in central Spitsbergen, the active layer thickness has increased more at locations on the west coast than in central parts (Etzelmüller et al., 2011). Measurements from the Spitsbergen side of Forlandsundet from 1996 to 2012 show great temporal and spatial variability in active layer thickness, dependent on landform/ site and year (Sobota & Nowak, 2014). For beach areas, an annual active layer thickness was measured to 124 cm whereas in tundra it was measured to 148 cm (Sobota & Nowak, 2014). The near-surface

temperatures on the Spitsbergen side of Forlandsundet have been estimated by Sobota and Nowak (2014) to have increased by more than 1.0°C compared to the 1970s. As the active layer thickness increases, slope stability may decrease in mountainous areas as the mass strength and cohesion is lowered (Masselink et al., 2011a), vegetation cover may be altered, and the release of greenhouse gases may increase (Sobota & Nowak, 2014).

Due to repeated thawing and freezing of the ground, geometric sorted patterns arises where the inner section comprises the finer fraction and is surrounded by coarser grained material (Gallagher et al., 2011) (Figure 2). Such landforms are named *sorted patterned ground* and are found in periglacial environments (Feuillet et al., 2021; Kääb et al., 2014). Sorted circles and sorted polygons are two subtypes that resemble each in appearance and size from a few cm and up to 4 m (Feuillet et al., 2021). Sorted polygons never develop individually (Feuillet et al., 2021).

Figure 2 Patterned ground. Extensive vegetation cover indicates old age of the ground cover. Location of photo: 78°32'46.01"N, 011°14'40.00"E.

2.3.3 Slope Processes

The term slope processes in geology essentially encompasses all physical processes that affect a material mass situated on sloped setting. This includes weathering, erosion transport and deposition of sedimentary material. The downslope motion of rock and/ or soils in a paraglacial environment also includes processes that are controlled by the

presence of glaciers, glacial deposits, the presence of permafrost and also the effects of climate (McColl, 2012).

The main driving factor is gravity (mass wasting) however other transport medium such as glacial ice, snow, or water (Harris et al., 1988a) also exert themselves in periglacial settings. Mass wasting is not restricted to the active layer, it can involve dislocation generated by the motion of ground ice in permafrost areas, e.g., landslides (Harris et al., 1988a). Common slope processes that have been identified on Svalbard include gelifluctuation, frost creep, debris flows and smaller landslides (Sollid & Christiansen, 2003), where the former two are examples on slow mass wasting processes and the latter on fast processes (Harris et al., 1988a).

Gelifluction and soil creep are terms of slope processes used instead of solifluction when freezing and thawing of the ground is controlling the downslope movement (French, 1996). *Gelifluction* is mass movement due to water-saturation of unconsolidated near-surface sediments that are underlain by a frozen base (Benedict, 1976). Gelifluction can occur due to melting of snow during spring or due to heavy rainfall. *Frost creep* is the net downslope movement that results as the particles in the ground expands perpendicular to the ground surface when freezing and settle vertically when thawing (Mayhew, 2009). Gelifluction and frost creep develop landforms like lobes and terraces (Benedict, 1976). Both types are examples of active-layer failure and are typical slope processes in areas underlain by permafrost. Other slope processes that involve failure of the active layer and permafrost, for instance retrogressive thaw slumps, are not regarded as active-layer failure (Harris et al., 1988a).

Meso-scale landslides that can occur in an environment dominated by permafrost include mudflows, mud slides and earth slides. These are displacement type processes that occur due to destabilizing of the ground as the thickness of the active layer increases and the near-surface sediments become waterlogged, as a result of heavy rain or snow melt (Mayhew, 2009).

Frost-wedging/ -shattering is a form of mechanical weathering (Lutgens et al., 2014b) that occurs on all scales where water trapped within a rock volume (e.g., within pore-spaces or fractures) expands during freezing, forcing mechanical exfoliation of the rock. This typically produces angular or blocky clasts as the rock is broken down along lines of natural weaknesses such as existing open-fractures or natural bedding surfaces (Figure 3).

Figure 3 Frost wedging/ -shattering interferes with beach deposits in Selvågen. Height of cliff is approximately 2 m. Location of photo: 78°32'46.01"N, 011°14'40.00"E.

2.4 Landforms

2.4.1 Gravel Beaches

Gravel beaches are coarse clastic shore-parallel deposits (Bluck, 2011). Movement along the shore occurs by wave action through asymmetric movement as uprush transports particles to the beach with an angle to the shore, and backwash transports sediment back perpendicular to the shore (Masselink et al., 2011c). *Selection pavement* is at an area in foreshore zone where swash and backwash sort sediments (Bluck, 2011). A mature selection pavement shows little variety in clast shape and size and indicates a high tidal range (Bluck, 2011). *Berms* are steep embankments which can be traced for tens of metres along the coast (Bluck, 2011). The berms represent the transition between the foreshore and the backshore (Figure 4) and is where waves break during storms (Oertel, 1985). The *backshore* is an area affected by overwash processes (Oertel, 1985). Just as the berms, the backshore consists of unconsolidated sediment (Oertel, 1985). Where big waves prevail, beaches typically show a steep incline towards the sea, illustrated in Figure 4, while beaches exposed to smaller waves have a shallower profile (Bluck, 2011).

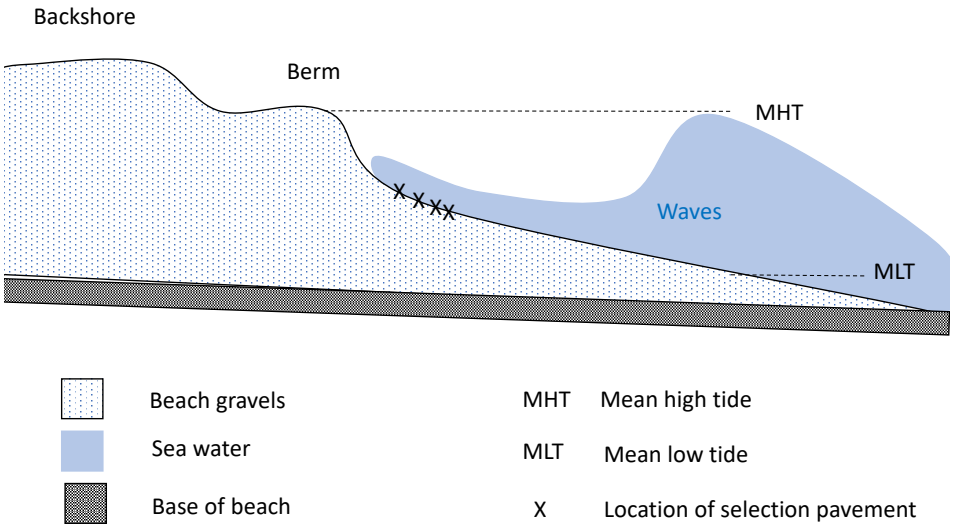

Figure 4 Characteristic features of beach deposits in a cross-section.

Gravel beaches can be found bordering river mouths where there is an extensive supply of sediments, in areas where cliffs supply sufficient amounts of sediments or they can have been built as former glacial deposits have been transported to the shore (Bluck, 2011). When the sediment supply to such beaches is sufficient, the beaches function as a protection shield to cliffs and prevent undercutting which is waves that erode cliffs from the bottom (Atkinson, 2005; Dickson et al., 2009). The characteristics of these beaches contain a steep incline towards the sea and usually a distinctive storm berm on the seaward side (Figure 4).

2.4.2 Barriers

A barrier can be defined as a shore-parallel depositional feature above mean high tide (MHT) that is separated from the mainland by e.g., a lagoon (Daniels, 1999; Otvos, 2012). Barriers differ from beaches by having a different morphology where the back-barrier dips toward land. It is an unconsolidated body of sand and gravel which separates the open sea from the inshore environment (Otvos, 2012), and can appear as a beach, spit, or chain. A barrier chain arises when inlets split the barrier and allow water to flow through (Daniels, 1999). Barriers are either barrier islands or mainland-attached barriers depending on connection to the mainland (Otvos, 2012). Barriers can be swash-aligned or drift-aligned which means deposits that are oriented parallel with the crest of the dominant incident waves or deposits that are oriented with an angle to the crest of the dominant incident waves respectively (Masselink et al., 2011c). Swash-aligned barriers show no longshore transport of sediment whereas drift-aligned barriers do and are thus susceptible to longshore drift changes (Masselink et al., 2011c).

Barriers as depositional features embody several landforms; beach, dune, shoreface, tidal delta, inlet, spit, and wash-over forms (Masselink et al., 2011c). They can form at wave-dominated, tidal dominated or mixed coasts, but the morphology is not dependent on which process that dominates (Mulhern et al., 2017). Barriers are elongated bodies that develop in length and height. The barriers increase in length by lateral accretion and progradation (Mulhern et al., 2019). They increase in height by storm waves that redistribute sediment and build up the barrier crest by wave overtopping (Avinash et al., 2013; Mulhern et al., 2019; Orford et al., 1991b). Storm-wave activity passes sediment over the barrier crest to the back slope of the barrier where it will be buried by successive wash-over sediment by storm waves. These deposits are shore-perpendicular lobes that incline towards land and are termed wash-over lobes (Masselink et al., 2011c; Orford et al., 1991a). As storm waves pass sediment onto the back barrier, the sediment that was once on the back slope will appear at the shoreline and thus be available for new storm-wave activity. The balance between overtopping and overwashing control the nature and pace of roll-over and migration (Orford et al., 1991b).

2.4.2.1 Coarse Clastic Barriers

Coarse clastic barriers are defined by Carter and Orford (1993) as depositional features that contain clasts which range in size from granules to boulders (Figure 5). Coarse clastic barriers can be found in previously glaciated areas, tectonically active areas where coarse material is brought to the coast by high-gradient streams or rivers, and at wave dominated areas where cliffs are exposed and prone to erosion (Van Rijn, 2013). These barriers are often found between headlands and adjoin cliffs or bluffs (Carter & Orford, 1993). Displacement and longshore movement of coarse clastic barriers occurs by wave action primarily.

The stability of such barriers largely depends on the quantity and continuity of sediment supply (Forbes et al., 1995a). According to Forbes et al. (1995b) stable coarse-clastic barriers appear as self-arranging as they involve "slow morphological, textural, and dynamic adjustments that operate to minimize entropy production". The slow phases can last from decades to centuries. The longer the slow phase lasts, the better the barrier will be to resist sudden and drastic external forces. When the barrier no longer can withstand the external forces, the stable structure of the barrier can be destroyed (Forbes et al., 1995b). The destruction or reorganization of the barrier occur relatively rapid and can take place over hours or days. Until the barrier has had the time to self-arrange, it can be denoted as unstable. An unstable coarse clastic barrier is typified by poor facies organization, low beach ridge crests, and repeated overwash processes that cut thru the

crests and form poorly sorted wash-over lobes on the back-barrier slope (Forbes et al., 1995b).

The climate is the main controlling factor when it comes to short-term changes for coarse clastic barriers (Forbes et al., 1995b) as a single storm event can impact the barrier´s stability and morphology. In a transgressive setting, the evolution of the barrier is determined by the preceding morphology and sediment supply (Forbes et al., 1995b). A landward migrating barrier can increase its migration speed by a single storm event, a general increase in storm frequency, or by a combination of the two (Forbes et al., 1995b). Migration can occur as a result of a single incident, or as a result of smaller incidents that occur successively (Forbes et al., 1995b).

When it comes to long-term development of barriers in a paraglacial environment, sediment supply still matters, but other factors control too. Relative sea-level change, coastal topography which includes geology and bathymetry, and climate regime are the three dominating controls (Forbes et al., 1995a).

Figure 5 Coarse clastic barrier. The clasts in the middle part of the photo are up to 30 cm in diameter. The photographer stands approximately 3 metres above MHT. From southern part of barrier in front of Richardlaguna, 78°47'51.09"N, 010°57'5.77"E.

2.4.3 Spits

Spits are supratidal depositional features prominent as ridges or embankments connected to land at one end and terminating in the open water at the other end (Evans, 1942). Spits are usually found where there is a sudden change in coastline direction or across bays (Masselink et al., 2011c) and evolve as longshore drift passes this sudden coastal change and the sediment supply is sufficient (Avinash et al., 2013). They are

narrow compared to length (Otvos, 2012) and can be up to several kilometres long (Stéphan et al., 2018). The spit stability depends on sea-level change, wave actions and sediment supply (Carter & Orford, 1993). These factors influence spit morphology too, as do longshore drift (Avinash et al., 2013), sediment supply (Avinash et al., 2013), and tidal and fluvial currents (Fisher, 1955).

Landward migration of spits due to rising sea level and/ or storm waves occurs as overwash processes take place (Avinash et al., 2013; Hequette & Ruz, 1991). Over time, spits can evolve into barriers and segregate an inshore environment from the sea. Some spits develop a branched tip due to refraction of waves or a strong tidal current, and such tips are called *recurved spits* (Masselink et al., 2011c) (Figure 6).

Figure 6 Spit in Selvågen. The photo illustrates how a spit typically looks. Three recurved spits at the end can be seen towards the west. Photo from 78°32'58.26"N, 011°15'6.00'E.

2.4.4 Tidal Flats

Tidal flats are coastal features that develop at slightly inclined shores and where tidal range is large relative to wave height (Friedrichs, 2011). Sufficient sediment supply and the absence of strong waves are crucial factors in developing a tidal flat (Reineck & Singh, 1980). Expansion of tidal flats occurs as the sediments supplied from land is kept in the nearshore area (Gao, 2019). Sediment grain sizes usually range from clay to fine gravel, and the finest fraction is found on the top (Reading & Collinson, 1996). Although tidal processes mainly control the tidal flat morphology, waves, biological processes (Gao, 2019) and winds from storms (Reading & Collinson, 1996) influence as well. Several characteristics are distinctive for tidal flats: mud draping, wave or oscillatory ripples (marked with orange circles on Figure 7), and channels that are located

perpendicular to the main flow direction (marked with dashed red line on Figure 7) as the whole channel network appears as a dendritic system (Dingler & Clifton, 1984; Hughes, 2012; Reading & Collinson, 1996).

Figure 7 Tidal flat in Selvågen. Wave ripples and a channel perpendicular to the main flow direction can be seen within the yellow and red circles respectively. Length of main channel is approximately 8 metres. Photo from 78°32'28.70"N, 011°14'5.49"E.

2.4.5 Alluvial Fans

Alluvial fans are fan shaped depositional features with a settled apex where the river emanate from upland. The active river channel shift position over time and hence the triangular shape is established. Transport processes within alluvial fans are debris flows, sheet flows and channelized fluvial processes (Harvey et al., 2005). Normally, the fluvial dominated fans are associated with lower gradients on the mountain side, while debris flows dominated fans are associated with higher gradients (steeper) (Kostaschuk et al., 1986). Fluvial dominated fans have several water channels which move laterally over time. Alluvial fans hold back most of the coarse sediments and thus control the supply of sediments to the lowlands. The appearance of alluvial fans is controlled by catchment characteristics which include drainage area, relief and lithology of bedrock (Mather & Stokes, 2018).

2.4.6 Colluvial Fans

Colluvial fans are deposits whose main transport mode is by gravity and less than 50% of the material is larger than pebbles (Parry, 2011). Transportation can also occur via water transportation in sheet erosion. Colluvial deposits tend to accumulate at the foot of slopes (Borradaile, 2014). The deposits are not sorted and consist of angular clasts.

2.4.7 Deltas

A delta is an accretion of terrigenous sediments partly above water deposited where the river mouth enters the sea or lake (Galloway, 1975). Morphologies of deltas depend on the interaction between fluvial and marine processes, and they are susceptible to change when internal factors, e.g., sediment supply, or external factors, e.g., wave height, change. Delta morphology depends on dominating regime, whether it is fluvial-dominated, wave-dominated or tide-dominated (Galloway, 1975). *Fluvial-dominated deltas* usually have great catchment areas and high river discharges into the sea where wave action and tidal processes are minor influences (Masselink et al., 2011b). *Wave-dominated deltas* are greatly prone to wave actions, but the sediment supply is however greater than the reworking and redistribution by waves (Galloway, 1975; Masselink et al., 2011b). *Tide-dominated deltas* have a greater tidal prism (defined by Hume (2005) as "the amount of water that flows into and out of a bay with the flood and ebb of the tide") than water supplied fluvially (Masselink et al., 2011b).

Although the delta morphology depends on the dominating regime, there are three main entities: delta plain, delta front and prodelta environment (Masselink et al., 2011b). Coarsening upwards is the usual trend when deltas prograde (Bhattacharya, 2006). The *delta plain* is the end of the river where it enters the sea. The plain has a very low gradient and can contain one or multiple channels on top. At the *delta front* fluvial-, wave-, and tide-processes interact, and the coarsest sediment load is deposited which leads to a seawards progradation if the wave- and tidal-processes allow (Masselink et al., 2011b). The delta front has a greater gradient than the delta plain (Masselink et al., 2011b). The last entity is the *prodelta*, the most seaward part, which can be located in deep water and up to several kilometres away from the delta plain, and hence, only the finer sediments are transported here to be deposited (Masselink et al., 2011b).

Another way to distinguish between different delta types is based on sediment grain size. *Fan deltas* comprise the coarsest clasts, primarily cobbles and boulders, and such deltas develop where subaerial fans terminate into the sea or where a river that is dominated by bedload transport enters into deep water (Masselink et al., 2011b). *Braid deltas* comprise finer clasts and usually better sorted the sediments as the clasts are

transported to the sea by a braided river (Masselink et al., 2011b). For the deltas that comprise coarse-grained sediments, the transport and deposition of sediments commonly occur by debris avalanches and flows.

3 STUDY AREA

The region of interest is the north-eastern coastline of Prins Karls Forland (Figure 1B & C). The topography of PKF is controlled by high alpine mountains in the north (highest mountain is Monacofjellet with a height of 1084 m) and a long coastal plain in the south. Coastal lowlands are present in front of the mountains. Small valleys are oriented approximately east-west transecting the island, most of which are ice free. The island is dominated by piedmont glaciers (Hagen et al., 1993) some of which terminate in the sea.

The eight study sites visited are labelled on Figure 1C. As the north-eastern coastline of PKF is a semi-open coast, the shoreline is exposed to swells and waves except in Selvågen where the bay is sheltered by bedrock headlands. The study sites have been divided into three regions with respect to the dominant geomorphology at the shoreline. The northernmost localities, the barrier complex in front of Richardlaguna, Fuhrmeisterstranda and Murraypynten, are dominated by coarse gravel beaches. The southernmost localities, Sessflya and Selvågen, are dominated by alluvium and colluvium The locations in the middle, in Brebukta, reflect the recent retreat of Søre Buchananisen and are dominated by glaciogenic sediment.

GLACIATION HISTORY

PKF has decreased in size from 626 km^2 in 1936 to 612 km^2 in 2008 due to melting of glaciers (Skinner, 2022). The glacial cover on Svalbard is ca. 60% today (Farnsworth et al., 2020) of 61,020 km^2 (NPI), but has been as little as 25% during Early and Middle Holocene (Farnsworth et al., 2020). The only glaciers that existed on Svalbard at that time were present in the north-eastern parts (Farnsworth et al., 2020).

It has been debated going when PKF was detattached from the Barents Ice Sheet that covered Svalbard during the Last Glacial Maximum (26,500 to 19,000 years BP) (Clark et al., 2009). Raised beaches left Salvigsen (1976) with the conclusion that Forlandsundet had not been covered with ice later than 40,000 years BP. This conclusion was also supported by considerable amounts of old sediments which Salvigsen (1976) believed would have been redistributed if a glacier had re-covered them. In contrast, Landvik et al. (2005) found that PKF was connected to the ice sheet which covered Spitsbergen even during the glacial minimum at Late Weichselian (at 13,800 years BP (Norðdahl & Ingólfsson, 2015). This was based on seismic data and supported by subglacial till deposits on the shelf west of PKF that correlate to till deposits outside of Kongsfjorden.

The findings of Landvik et al. (2005) were supported by Butschek et al. (2019) who stated that Forlandsundet was fully glaciated during the Last Glacial Maximum and hence PKF was connected to the ice sheet that covered Spitsbergen.

The change to an interglacial period occurred over a relatively short amount of time (Landvik et al., 1998). The Holocene glaciations continued the work of Pleistocene glacials in shaping the topography of Svalbard. Most of Svalbard´s glaciers that exist today initially started to develop 5,500 years ago (Fjeldskaar et al., 2018). These glaciers have reached their greatest extent twice; approximately 2500 years ago and at the end of the Little Ice Age (at ca. 1920) (Svendsen & Mangerud, 1997).

During the last 15,000 years there have been three high sea-level events on Svalbard where the first is linked to deglaciation of the Barents Ice Sheet (Forman, 1990). Then the eustatic sea-level rise was exceeded by uplift and unloading due to the deglaciation. This lead to a forced regression on the western parts of Spitsbergen (Forman et al., 2004). The next two sea-level rises occurred during the Middle- and the Late Holocene, where the former appeared around 5,500 years ago and the latter around 2-1000 years ago (Forman, 1990). The latter sea-level rise eroded former raised beaches. Today, Svalbard experiences uplift and there is a big span in the degree of uplift within the archipelago. The greatest degree of isostatic uplift occurs in the eastern and central parts of Svalbard. PKF experiences an uplift of 4.3 mm (NRK, 2022).

BEDROCK

The bedrock of PKF consists of a metamorphic basement that spans most of the island but is locally covered by a younger sedimentary succession. The metamorphic basement consists of Neoproterozoic rocks which generally exhibit greenschist facies. The sedimentary deposits comprise Paleogene rocks deposited in grabens of the large-scale Hornsund Fault Complex (Dallmann, 2020), and they are exposed locally along the northeast coast of PKF. The oldest sedimentary rocks deposited in the graben are conglomerates which are estimated to be of late Eocene to early Oligocene age (Dallmann, 2020). These are found in Selvågen. Generally, the graben contains repeated successions of clastic deposits that consist of polymict conglomerates, sandstones, siltstones and claystones (Dallmann, 2015), all of which can be found along the east coast of PKF. These deposits are quite small in extent and thickness, and partly overlap each other (Dallmann, 2020).

OCEANOGRAPHIC INFORMATION

An extension of the Gulf Stream, the Norwegian Atlantic Current, provides the Arctic Ocean with warm water (Kejna & Araźny, 2012; Smedsrud et al., 2022; Svendsen et al., 2002) (Figure 8). The branch that flows past PKF is called the West Spitsbergen Current which is a continuation of the Norwegian Atlantic Current (Figure 8). The temperature of the Norwegian Atlantic Current has risen since the 1970s (Smedsrud et al., 2022; Svendsen et al., 2002), and so has the temperature of the Arctic Ocean (Smedsrud et al., 2022). Smedsrud et al. (2022) found that the North Atlantic Current brings greater volumes of water than it did 50 years ago due to stronger winds and an increased density contrast between Atlantic Water and the cold water in the Arctic Ocean.

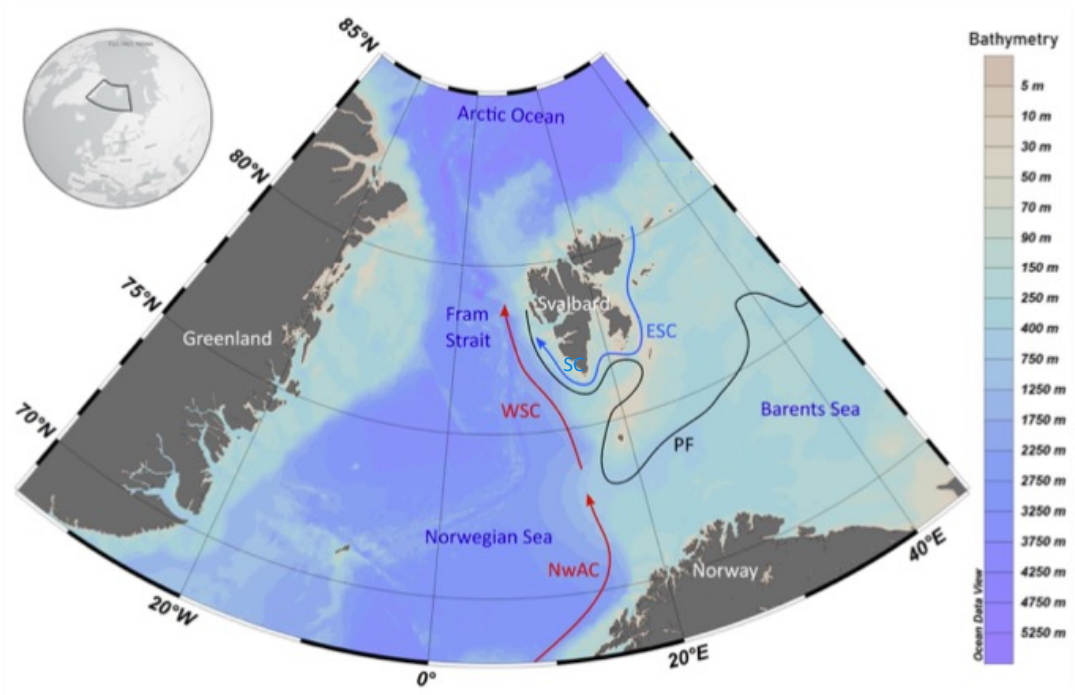

Figure 8 Oceanic circulation pattern around Svalbard. The West Spitsbergen Current (WSC) is a continuation of the Norwegian Atlantic Current (NwAC) and supplies the Arctic Ocean with warm water. PF: Polar Front. Figure courtesy of Missana (2021).

The West Spitsbergen Current influences the climate at PKF through air temperature (Smedsrud et al., 2022; Walczowski & Piechura, 2011) which ultimately dictates cloud density and hence precipitation rates (Kejna, 2012). Erosion by waves during winter is indirectly influenced by ocean currents as the extent of sea ice cover is a response to the oceanic temperatures (Walczowski & Piechura, 2011). The West Spitsbergen Current is not the only ocean current that influences PKF, so does the cold Sørkapp Current that is a continuation of the East Spitsbergen Current which originates east of Svalbard (Kejna, 2012) (Figure 8). The Sørkapp Current can bring substantial amounts of sea-ice chunks into Forlandsundet (Kejna, 2012). Forlandsundet is open throughout the entire winter

now but used to be frozen during winter until the 1970s according to the local Stig Henningsen at Henningsen Transport and Guiding in Longyearbyen.

Although the dominant wave fetch at PKF is from the southwest (Klemsdal, 2010), the east coast experiences swells from both the north and the south as the swells are channelized through Forlandsundet. Wind generated waves can build up across Forlandsundet. The deepest point at the shallowest area in Forlandsundet is 3 metres. This point is located west of Sarstangen and east of Murraypynten (Figure 1B&C). Tidal height is around 1 m (Bourriquen et al., 2016), and the tide is semidiurnal (Kowalik et al., 2015).

CLIMATE

The climate on PKF can be categorized as a High Arctic maritime climate (Eckerstorfer & Christiansen, 2011). From November to May the climate is dominated by Siberian Highs, extremely harsh and cold weather conditions, that alternate with Icelandic Lows, airflows that lead to snowfall, warmer temperatures and even melting during winter (Sollid & Christiansen, 2003). The mean annual temperature has increased by 1-2 °C from the early 1980s to 2010 on Svalbard (Førland et al., 2011). The temperature increase is however not evenly distributed throughout the year; summer temperature on Svalbard has risen 0.5-1.0°C and winter temperature has risen 3.5°C (Førland et al., 2011). The mean annual air temperature measured in Longyearbyen from 1971 to 2000 is -5.6 °C (Hanssen-Bauer et al., 2019).

There have been few meteorological studies on PKF, and those which have been carried out have only been investigating through one or two summer seasons (Kejna & Araźny, 2012). The annual precipitation varies at different locations on Svalbard, but there is an overall increasing trend (Førland et al., 2011). In Ny-Ålesund, Kongsfjorden (Figure 1B), the average annual precipitation is twice as high as at Svalbard Airport, Isfjorden (Førland et al., 2011) where it has been measured to be 196 mm in the time period of 1971 to 2000 (Hanssen-Bauer et al., 2019). The closest precipitation measurements come from Ny-Ålesund where 400 mm is the yearly average. (Hanssen-Bauer et al., 2019).

The prevailing wind direction on Svalbard is from the southeast during winter time (Humlum et al., 2007), while during summer the prevailing winds come from the west (Sollid & Christiansen, 2003). The wind speed is higher during winter time, generally 5-20 m/s, compared to summer time where the wind speed generally is 1-8 m/s (Humlum et al., 2007).

With regards to storminess, the Circum-Polar Region within which Svalbard lies usually displays a quiet spring and summer trend and an increase during autumn (Atkinson, 2005). July is the month with the least storm activity and the weakest winds, while October displays the strongest storm and wind pattern (Atkinson, 2005). While Serreze et al. (1993) stated that the storm activity in the Arctic had shown a steady increase from 1950 to 2000, both Atkinson (2005) and Savelieva et al. (2000) found that there were distinct periods with different trends within the main increasing trend. A 20-year period of storm-activity decrease came first, which was followed by a high intensity period of a couple of years and then a continuity of increased storminess. Atkinson (2005) and Savelieva et al. (2000) agree that the most evident changes between these periods arise as a result of alterations in large-scale atmospheric circulation systems.

PERMAFROST DEPTH

No studies have made on either permafrost depth or the active-layer thickness on PKF. The closest study on active-layer thickness has been carried out on the Spitsbergen side of Forlandsundet (at Kaffiøyra). The thickness was measured to be 124 cm in beach deposits (Sobota & Nowak, 2014).

4 METHODS

Fieldwork took place at the north-eastern coastline of PKF from September 4th to 13th 2021 as part of a coastal mapping project with focus on geomorphology and sedimentary systems on Svalbard. Fieldwork was carried out to gather on-site information and knowledge to obtain a complete understanding of the mechanisms and processes that dominate the coastline.

4.1 Fieldwork

Geomorphological work was carried out in selected areas shown in the white boxes in Figure 1C. Detailed maps are shown under each section under results. The importance of being present in the field cannot be stated clearly enough, as first-hand knowledge and observations are essential to identify all the processes and landforms at the study sites. The processes influencing or dominating the coast could not have been determined by examining satellite images only, nor could the landforms that are present or grain sizes that compose the landforms.

An iPad with the map-based program Field-Move was used as a tool for mapping. Accuracy of the iPad GPS is 30 m (GeoSpatialExperts). A handheld Garmin GPS was used to map the border between land and sea and the boundary was set to MHT. This was achieved by walking along the current high-tide wash mark. Such tracks were made along the coast from the southernmost and northernmost parts on the barrier in front of Richardlaguna (Figure 9), and from Fuhrmeisterstranda and almost down to Murraypynten. Instrument accuracy of the handheld GPS is according to Garmin within 15 m 95% of the time, and normally within 5 to 10 m (Garmin).

Figure 9 Present-day high-tide swash mark at southern part of the barrier in front of Richardlaguna. Location of photo: 78°48'6.83"N, 010°56'57.08"E.

4.1.1 Relative Age Dating in the Field

Relative dating of landforms in the field helped in getting a better understanding of the coastal evolution. This was based on the presence or absence of vegetation and moss, comparing areas with more vegetation relative to other areas if vegetation was present, distance to the sea, height of landforms above MHT, orientation of landforms compared to each other, or on the presence of whale bones or logs on landforms. These factors in combination aided in determining the evolution, the active parts, and relative ages of landforms.

4.1.2 Sampling

Sedimentological descriptions of morphological elements were made at locations shown in Figure 10 and three identifying factors were emphasized. *Grain size distribution* is based on minimum, median and maximum grain size, and is given in cm or descriptive terms given in Table 1 if stating the exact value was difficult. Classification of *roundness* includes very angular, angular, sub-angular, sub-rounded, rounded, and well-rounded. As for *sphericity*, the classification includes only three groups: low, medium, and high.

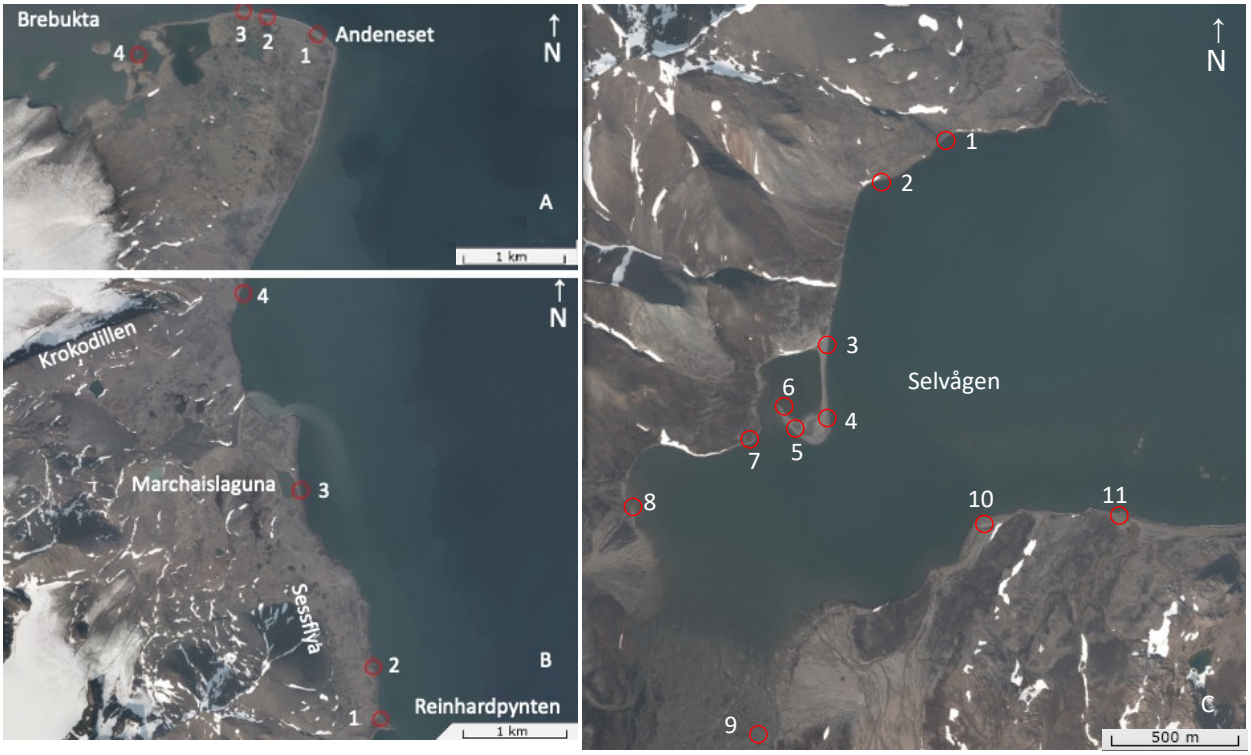

Figure 10 Locations of grain descriptions. Background satellite image courtesy of NPI.

4.1.2.1 C-14 Sampling

Samples for dating the beach deposits were gathered from logs, whale bone remains and shell fragments. Table 2 shows location, height above sea level and type of burial for the respective samples and on which landforms they were situated. Most of the items were partly buried under either vegetation, at most 2.0 cm thick cover, and/or rocks. The whale bone sample from Richardlaguna was the most degraded sample. The objects collected for sampling were chosen because they were representative for the coastal evolution. Samples 1-7 were sent to National Laboratory for Age Determination at the Norwegian University for Science and Technology (NTNU) for analysis.

Table 2 Samples for C-14 dating

Object		Position			m above MHT	Burial	Landform
1	Shell fragments	Murraypynten	78°43'58.68"N	011°09'0.42"E	1 m	15-20 cm down	Coastal lowland/ dried lagoon
2	Log	Andeneset	78°37'1.33"N	011°15'30.98"E	1.5 m	Partly buried	Beach deposit
3	Whale bone	Richardlaguna	78°46'23.82"N	011°02'21.35"E	1.5 m	Partly covered by vegetation	Beach deposit
4	Log	Murraypynten	78°43'31.83"N	011°08'50.30"E	Ca 1.2 m	Partly covered by vegetation	Beach deposit
5	Log	Richardlaguna	78°46'14.42"N	011°04'10.29"E	1.5	No burial	Beach deposit
6	Whale bone	South of Fuhrmeister-stranda	78°44'36.60"N	011°09'13.83"E	Ca 1.5 m	Partly covered by rocks	Beach deposit
7	Log	Richardlaguna	78°49'11.71"N	010°59'7.18"E	Ca 1 m	Partly covered by rocks	Beach deposit

Figure 11 Sampled log. The photo illustrates vegetation cover and degradational stage of object. From Murraypynten, 78°43'31.83"N, 011°08'50.30"E.

4.2 Post-Fieldwork

4.2.1 Investigation of Aerial Photos and Satellite Images

The geomorphological and surficial sedimentological maps were made by using ESRI ArcGIS Pro 10.7. The maps have been projected in the ETRS 1989 UTM Zone 33N coordinate system. Aerial orthophotos provided by NPI from 2008 have been used as a basemap. The maps produced are based on field observations compiled with satellite images from NPI (from 2008) and Petroleum Experts (from 2021). Geomorphological features present in the landscape have been mapped in ArcGIS Pro with cartographic symbology and colour-coding following the standard of the Geological Survey of Norway (NGU). The area has been mapped at 1:30 000 but the maps are presented herein at 1:50 000. The zoom level while mapping in ArcGIS Pro was set to 1:3000.

Oblique aerial photos from NPI taken in 1936 have been used to get an understanding of the retreating glaciers after the end of the Little Ice Age. Other than the aerial photos, all photos were taken by the author unless otherwise stated.

4.3 Errors Connected to Field Work and Post-Field Work

4.3.1 Errors connected to post-fieldwork and C-14 dating

There are some uncertainties with the dating of logs and whale bones and direct linking between the age and the landforms. Logs can have been used for building materials for cabins and could be a lot older than the beach deposit, the logs could be moved by humans after the cabin had collapsed, or the log could be put at its location a long time after the beach deposit was created. The whale bone remains do most likely not come from whales that died at the exact time when the beach deposit formed, as the deposit formed over a longer time. The whale bone remains have been washed onto the shore after the whales died and depending on how long the dead whales stayed in the water or at other beaches before it ended where it did, the dating error can be significant. Also, the past wave action strength can influence and give deviation from the correct age. If the wave action was very strong at the time when the dead whale was floating around, the whale bones could have been washed far inland, and hence give the impression that the beach deposit which the bones landed on, is younger than it actually is.

5 RESULTS

The results presented below are based on the observations and measurements made in the field in combination with aerial photos and satellite images provided by NPI. The geomorphological and surficial sedimentological maps are presented at the end of each section described.

5.1 Coarse Gravel Beaches

Figure 12 Map showing the northernmost localities. The barriers in front of Richardlaguna, Fuhrmeisterstranda and Murraypynten consist of similar beach deposits. Map courtesy of NPI.

The beach deposits that compose the shoreline from Heemskerckneset and southwards to Murraypynten (Figure 12) are very much alike. They are similar in size, shape, and landform appearance. All are unconsolidated. Bedrock is visible at some parts along the coastline, especially at Fuhrmeisterstranda where the beach deposits are located in front of 1 – 5 m high cliffs. Otherwise, the terrain is flat behind the coast.

HINTERLAND

The hinterland of Richardlaguna is mountainous with several small rivers that drain the area before they enter the lagoon. In front of the mountains a flat area at less than 100 metres altitude, a coastal lowland, is situated. Rivers and streams run over the coastal lowland. Two small glaciers, Vesalbreene (Figure 12), provide glacial meltwater and glaciogenic sediments to the lagoon. Glaciogenic sediments are provided from the moraine of Murraybreen to the Richardlaguna and Murraypynten areas. There are no streams or channels from the moraine of Murraybreen to Fuhrmeisterstranda, only drainage channels from small lakes enter the sea at Fuhrmeisterstranda. The small lakes are located on a vegetation covered plateau that is around 10 m above sea level and the draining channels incise the otherwise flat terrain. The plateau borders the beach deposits with cliffs at the northern parts of Fuhrmeisterstranda, while further south a gentle slope towards the beach deposits is present. The area behind Murraypynten is relatively flat and of low altitude, less than 25 m, with small lakes behind the beach deposits. There are no connections to the open sea today.

TIDAL INLETS/ OPENINGS

The number and locations of openings of the barrier complex have changed over the last 85 years. By studying aerial photos from 1936 provided by NPI, two openings were present at that time (Figure 13). One opening was far south, close to Rottenburgpynten, and the other was a few hundred metres south of Heemskerckneset. Satellite images from 2008 show only one opening while in 2021, the number of openings had changed back to two (Figure 14). The openings recorded in 2021 are located at 78°48' 11.11"N, 010°56' 48.18"E and 78°48'37.53"N, 010°57' 43.03"E. The latter is 450 m north of the opening which existed in 2008.

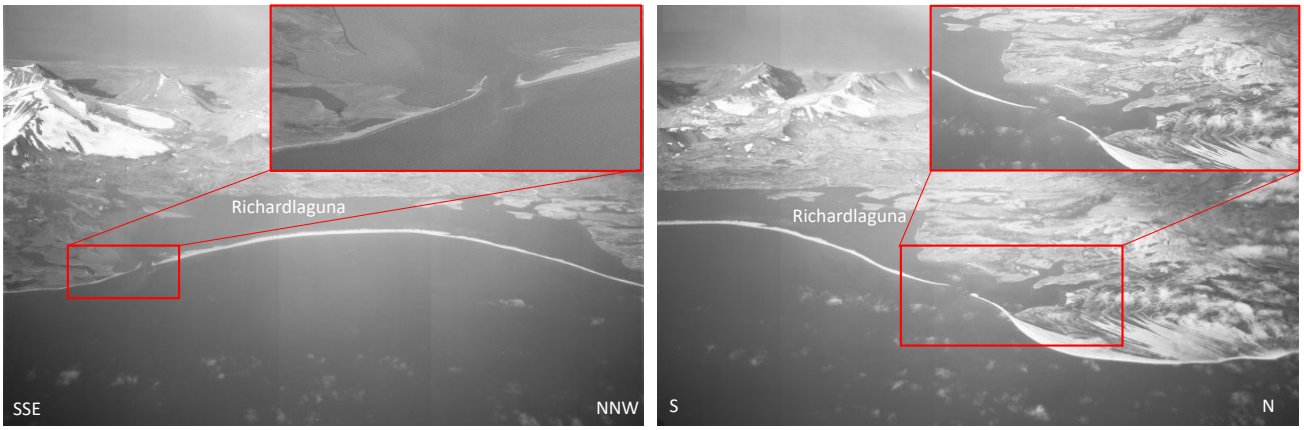

Figure 13 The barriers in 1936. Background photo courtesy of NPI.

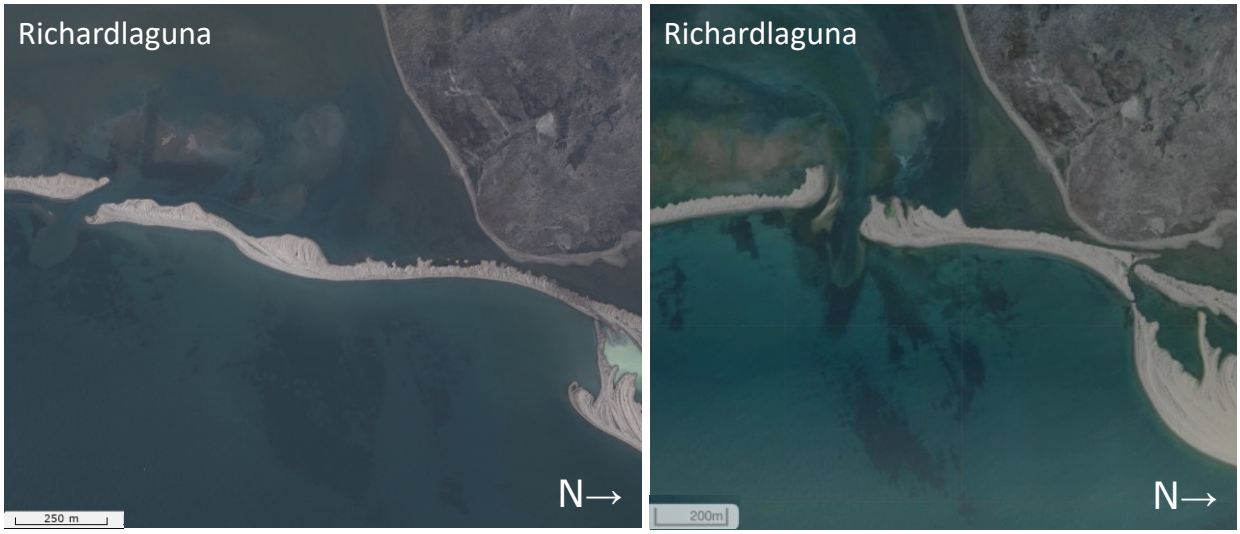

Figure 14 Tidal inlets/ openings of the barrier complex in 2008 (left) and 2021 (right). Background satellite images courtesy of NPI (left) and Petroleum Experts (right).

Another striking difference from 1936 to today is the distance between the barrier complex and the mainland in the northernmost part (Figure 13 & Figure 14). The barrier has moved landwards over the lagoon between 1936 and 2008 (Figure 14). The landward segment of the barrier is composed of overwash and overtop sediments that have been moved from the foreshore and nearshore area during storms. A comparison of Figure 13 & Figure 14 does not only show barrier migration but also change of the barrier width. The northern part of the barrier complex is 340 m at its widest today, while in 1936 the barrier was narrower.

Lakes enclosed by beach deposits are located at the southern end of the barrier complex (Figure 13) and close to Murraypynten (Figure 15, Figure 23). The lake at the barrier complex had no connection to the sea in 1936, while at Murraypynten the lake had an opening which is closed today. In the area near Murraypynten, several lakes were and are still present (Figure 23). North of the headland, a broad zone of weathered material with a high content of boulders (Figure 23) separates the lake with the former opening and a nearly dried out lake. The nearly dried out lake appears as a complete lake on the map (Figure 12) but it is not. Here, wet sand and mud with shell fragments are found in circular formations of 2 metres surrounded by bigger and angular rocks. The C-14 sample with shell fragments is from one of these circles. West of Murraypynten headland, another dry lake is present. This lake had no connection to the sea in 1936 (Figure 15), but the border of this lake showed sorting of grains and no vegetation as was the case for the nearby area.

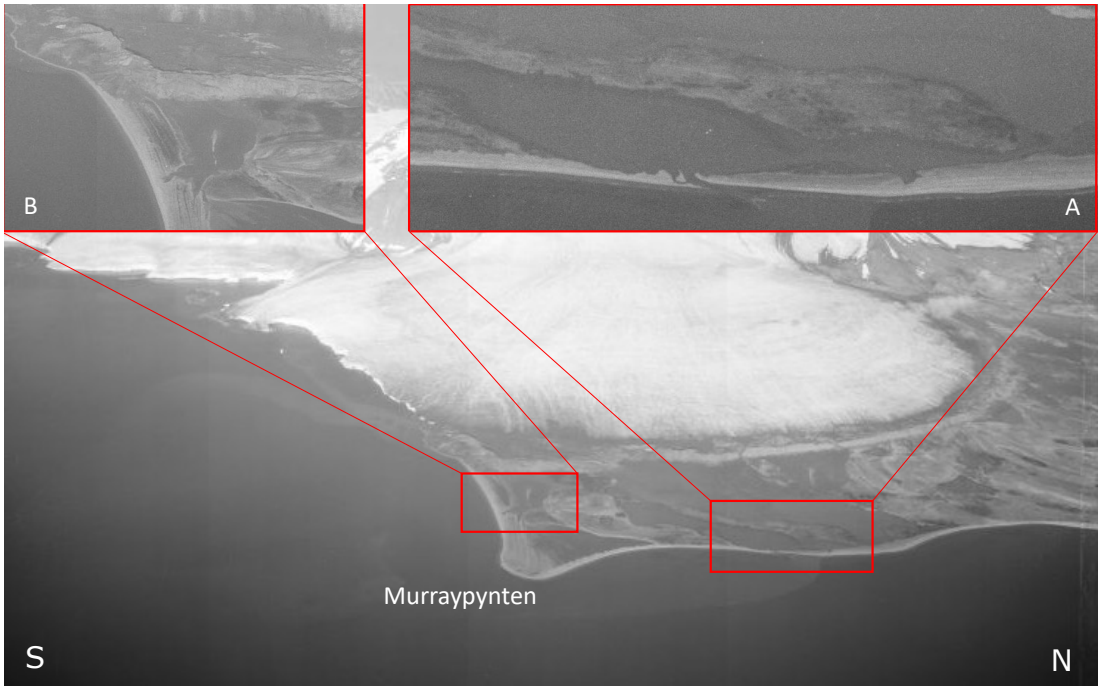

Figure 15 Lagoon (A) and lake (B) at Murraypynten in 1936. Background photo courtesy of NPI.

STRUCTURE

The total length of the beach deposits from Heemskercknesset to Murraypynten is 12.5 km, where 7 km constitute the barrier complex. The width of the barrier complex varies from 150 m to 340 m in the northern part while further south the maximum width is a few tens of metres. The beach deposits consist of several embankments or ridges separated by distinctive crests and troughs between, where the crest height varies from 1 – 3 m above MHT. The highest crests are found at the barrier complex where the ridges are up to 3 m above MHT. The crest height decreases towards Murraypynten where maximum crest height above MHT is 1.5 m. Following the coastline west of Murraypynten, the crest height is even lower.

The embankments or ridges are curved (Figure 16 & Figure 17). While the ridges on the northern and middle part of the barrier complex curve towards the southwest, the ridges on the southern part appear to curve towards the northwest. Where the arrows are pointing on Figure 17, the ridges terminate. The ridges flatten where they terminate. The southern parts of the barrier complex have older ridges on the back-barrier side that are not exposed to modern wave processes (Figure 16, bottom left).

Figure 16 Ridge direction. The innermost back-barrier ridges on southern part (highlighted in bottom left image) of the barrier complex show a different orientation than the outermost ridges (highlighted in top left image). Background satellite images from 2008. Images courtesy of NPI.

Figure 17 Direction of ridges that compose the barrier complex, 2021. Ridges terminate at the end of the arrows. Background satellite image courtesy of Petroleum Experts.

The curving ridges that originate along the seaside of the barrier complex create a shore-parallel ridge (best illustrated on the southern and middle parts of the barrier complex in Figure 17). A tidal delta is present on the landward side of the tidal inlet (best seen in Figure 17). The beach ridges along Fuhrmeisterstranda do not curve as much as at the Barrier, they rather follow the cliffs. Some curving is however present, but to a lesser extent. At Murraypynten, the beach ridges are parallel with the coastline even when they bend around the headland.

As mentioned above, the northern part of the barrier complex is less structured than the middle and southern parts and even small lagoons are found within the barrier (Figure 17, top part). In addition, ridges that curve towards land merge at some places within the barrier complex (Figure 18). These landward curving ridges terminate in a ridge that forms the border of the beach deposits to the lagoon (Figure 19).

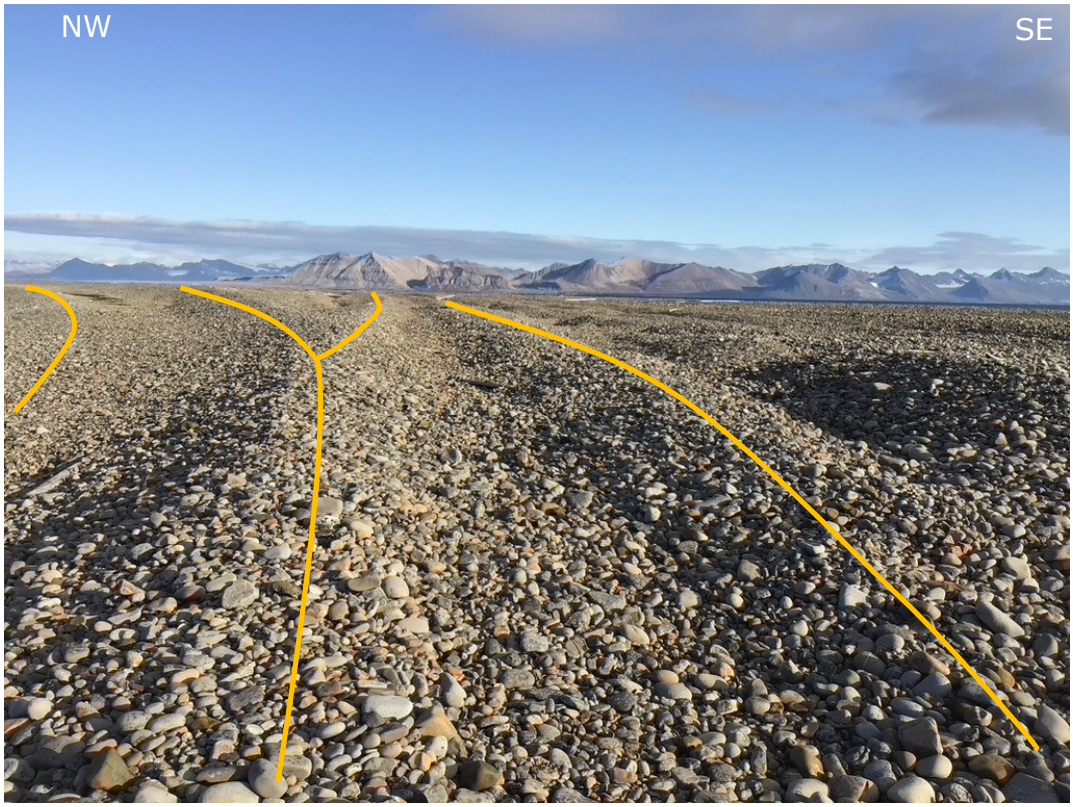

Figure 18 Merging ridges. The crests of the ridges are marked with yellow and correspond to the ridges marked with yellow in Figure 17. Photo from the northern part of the barrier complex, 78°49'12.95"N, 010°59'14.14"E.

Figure 19 Ridges on the landward side of the barrier complex. The crests of the ridges marked with yellow correspond to Figure 18, curve towards land and terminate in the ridge marked with red. Photo from the northern part of the barrier complex, 78°49'12.95"N, 010°59'14.14"E.

INSHORE ENVIRONMENT

Rivers and streams that drain the mountainous hinterland of the lagoon or originated from glaciers enter the lagoon. Most of these water channels are in the southern end closest to glaciers (Vesalbreene) and glacial material. Small beaches confined within bedrock are found on the mainland side of the lagoon. Where the barrier complex consists of distinct ridges on the landward side (Figure 19, Figure 23), the ridges have a steep side that faces the lagoon and even show signs of erosion as the ridge crest curves along the length of the ridge.

WASHOVER DEPOSITS

Erosive edges were present on the seaward side of the beach ridges and wash-over lobes prevailed on the landward side throughout the beach deposits. The wash-over lobes stretched up to 15 m inland, dipped towards land at around 10° and coarsened outwards. The wash-over lobes were present next to each other and thus left the crest of shore-parallel beach ridge curved. The wash-over deposits partly covered bedrock in the southern part of the barrier complex. At Murraypynten these wash-over deposits were underlain by angular and vegetated deposits.

GRAIN SIZES

The deposits that compose the barrier complex contain well-rounded, unconsolidated clasts on the surface that range in size from a few cm to 30 cm. The biggest clasts were observed above the MHT and not on the surface of the tidal area. The clasts that compose the coastline from Heemskerckneset to Murraypynten resemble each other in size, colour, and degree of roundness and sphericity. No lateral sorting was observed.

At the southern end of the barrier complex and next to Murraytjørnene where bedrock is present close by, the deposits that composed the barrier and beach were angular. In addition, a big boulder with a diameter of 1.5 m was present in the most landward part of the barrier complex at the southern end (Figure 23).

Within an erosive cut through the top part of the barrier complex, finer material than what is at the surface was observed (Figure 20). The cut was at ca. 2 m above MHT. The total height of the cut was 60 cm where the lowermost 25 cm consisted of coarse gravel to pebbles without matrix. Within this first division, at 15 cm, gradually more sand was present. Then the next 10 cm consisted of medium to coarse sand with coarse pebbles in between. The top 25 cm was clast supported where the sizes of the clasts ranged from 2 to 10 cm in length. The sorting is poor. The roundness and sphericity of the matrix was poor. This cut was one of many and hence gave the crest of the shore parallel ridge a curving appearance. Behind these cuts wash-over lobes were present.

Figure 20 Erosive cut. The person and the cut are above MHT. From the barrier complex, 78°47'27.20"N, 010°57'28.03"E.

VEGETATION

Vegetation (moss and lichen) was found on beach deposits furthest away from the shoreline. At the barrier complex, the vegetation extent was most pronounced in the northern parts where approximately 10-20% of the beach deposits were covered. Near the vegetated rocks, others had weathered and cracked into thin layers. This was not the case for the southern or middle part of the barrier, as hardly any vegetation or moss was observed and no or very few rocks had weathered.

Beach deposits with little vegetation were observed along Fuhrmeisterstranda, while at Murraypynten more clasts had more vegetation on (Figure 21). A Murraypynten, a surface transect of 42 m was made from MHT to the landward border of beach deposits. This transect can be divided into three areas with respect to vegetation. Unvegetated clasts are closest to the sea, a transition area with vegetated clasts overlain by unvegetated clasts is in the middle, and vegetation covered clasts are located furthest away from the sea. The unvegetated area is 25 m wide and composes ca. 60% of the total length, the transition area is 6 m and ca. 14% of the total length, and the vegetated area is 11 m and constitute the remaining 26% of the transect.

Figure 21 Beach deposits with extensive vegetation cover. From Murraypynten, 78°44'00.4"N, 011°10'14.60"E.

ORIENTATION OF BEACHES AT MURRAYPYNTEN

Less than 100 m west of Murraypynten beach ridges with a different orientation to the modern ones are situated 25 m inland from the shoreline (Figure 22). The old deposits are oriented E-W and have curving ends towards SE. The modern deposits bend from around Murraypynten and seem to cut through the old ones. The old beach deposits consist of ridges with clear crests and troughs between them. The overall height above MHT is higher than the modern deposits, but the crests' height is lower than that of the crests of the modern deposits. The older beach deposits have a smaller range of grain sizes, the biggest clasts are smaller too, and have lower sphericities than the modern deposits. The vegetation cover of the old deposits is dense, approximately 80% is covered while the modern deposits have no vegetation at all. Between the old beach ridges and the modern ones, transitional ridges are present. Some of the clasts in the transitional area are covered with vegetation. The un-vegetated clasts are deposited in lobe-shaped patterns which stretch 10 m inland from the modern beach deposits.

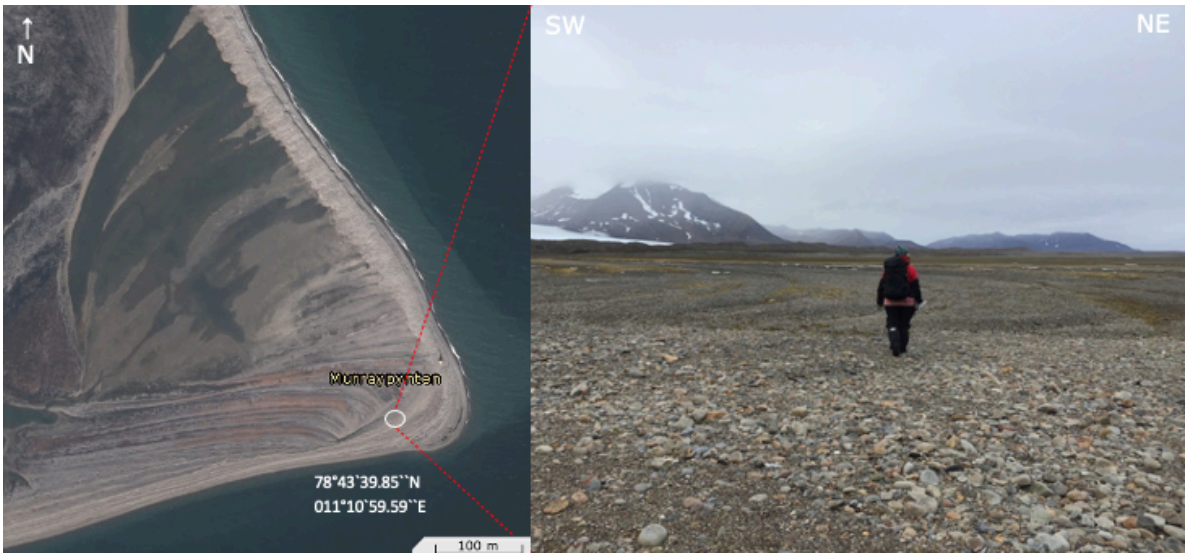

Figure 22 Old beach deposits. The different orientation is illustrated with the satellite image and the photo. Location of photo is 78°43'39.85"N, 011°10'59.59"E. Background satellite image courtesy of NPI.

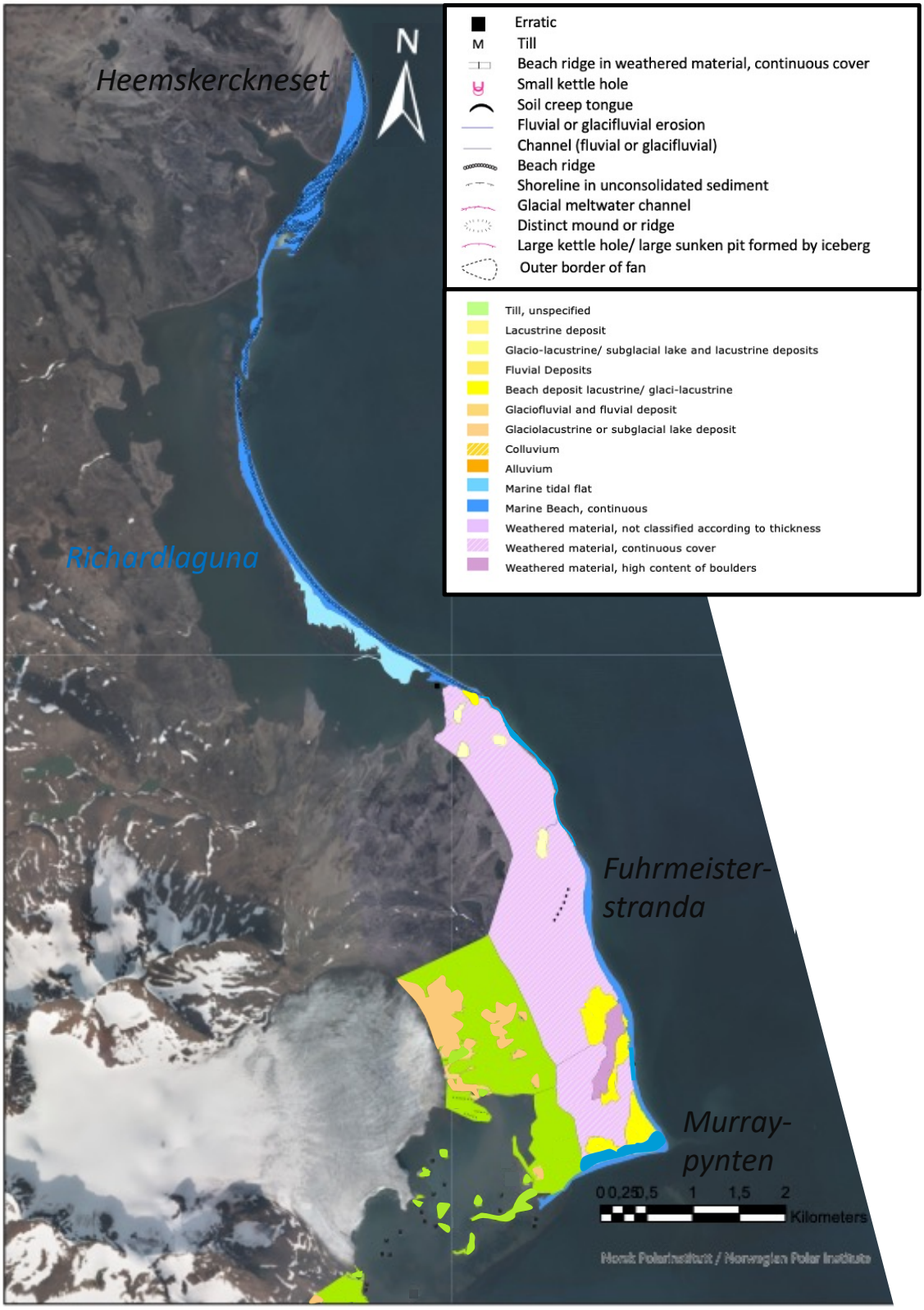

Figure 23 Geomorphologic and surficial sedimentologic map (Quaternary map) over the northernmost localities. Background satellite image courtesy of NPI.

5.2 Glaciogenic Deposits Dominated Coast

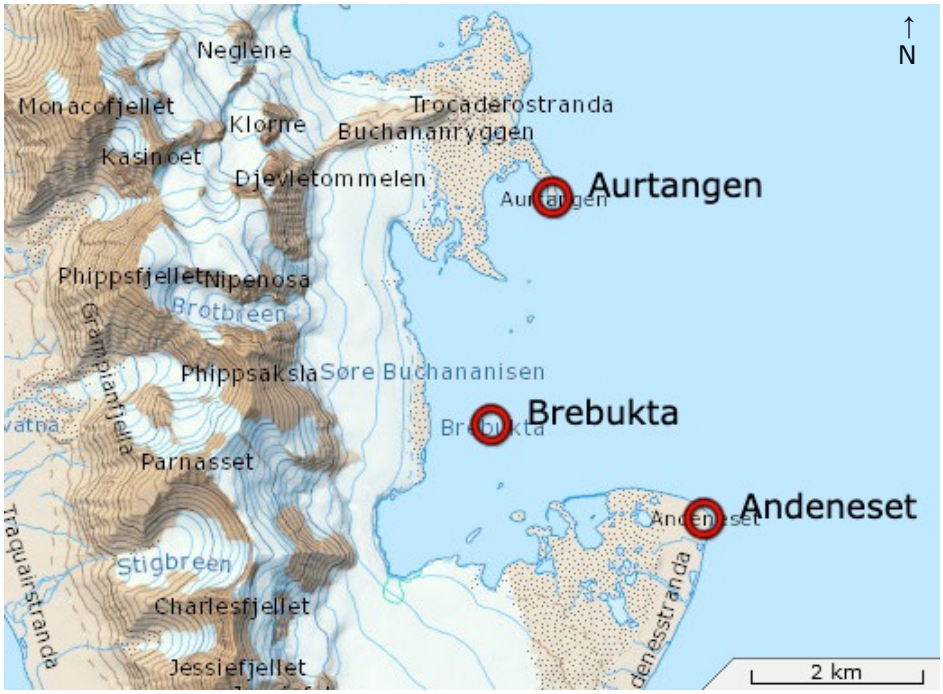

Figure 24 Map showing the midst localities. Aurtangen, Brebukta and Andeneset are under the influence of the previous glacial extent of Søre Buchananisen. Map courtesy of NPI.

The coastal area from Aurtangen to Andeneset is covered with extensive amounts of moraine material (Figure 24). Only Andeneset and the tip of Aurtangen were ice free in 1936 (Figure 25, Figure 26). Glaciogenic sediment is also present in the sea. Aerial photos from 1936 show a much greater extent of Søre Buchananisen than today (Figure 25, Figure 26). The southern part of Søre Buchananisen contributes with sediments to the shore through calving, which was observed numerous times during the fieldwork, and through meltwater.

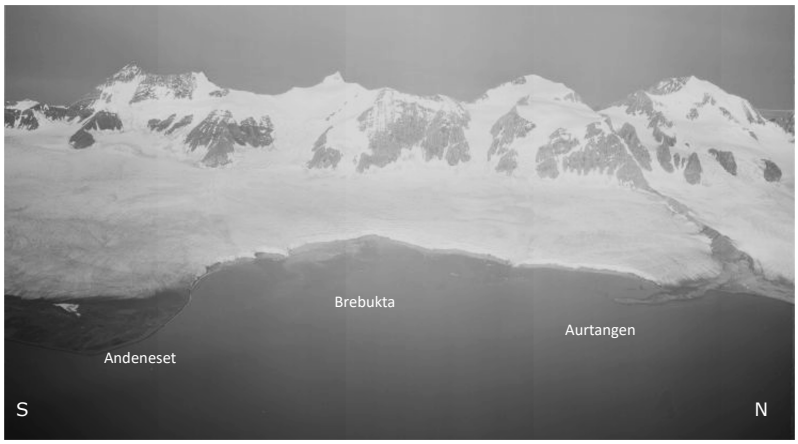

Figure 25 Brebukta with surrounding headlands in 1936. Background photo courtesy of NPI.

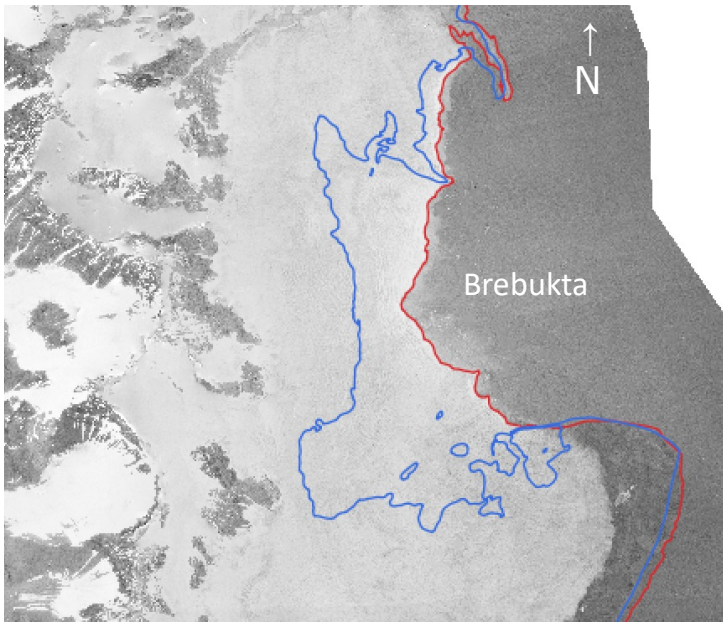

Figure 26 The shoreline in Brebukta in 1936 (red) and 2008 (blue). Figure from Skinner (2022).

The coast near Aurtangen is a disorganized area with distinct bedrock outcrops within deposits of glaciogenic sediments in all shapes and sizes, and small beaches. Where bedrock is present, beaches have not developed at all or to a very small extent and hence the bedrock constitutes the shoreline. A small, elongated lagoon is present in the innermost part of the bay and is confined by bedrock and glaciogenic deposits (Figure 27). Logs up to 3 m long were found on the landward side of the lagoon. Wash-over lobes up to 50 cm in length were seen on the beaches inside the lagoon. Small, dried-out channels cut through the wash-over lobes.

Figure 27 Disorganized coast and shore at Brebukta, near Aurtangen. The lagoon is elongated and has an uneven border. The photo is a composite of two photos taken at 78°39'7.23"N, 011°08'13.70"E.

Bedrock is not only visible along the shoreline at certain sections, but also exposed in the sea where it is overlain by moraine material. The deposits appear in bow-shaped formations (marked with green on Figure 28). The bedrock and/or moraine material located in Brebukta is exposed to incoming waves both from the south and from the north. The moraine material functions as obstacles for the waves, making the waves refract and lower their energy. Some of the boulders are above MHT while the existence of others can only be known from waves breaking on them during low tide.

Figure 28 Moraine material in the sea. The green line indicates the crescentic position of the moraine material in the sea. Moraine material is also present at the headland itself. From Aurtangen, 78°39'1.76"N, 011°09'51.23"E.

The Aurtangen cape is covered with moraine material and is highly exposed to incoming waves both from the north and from the south. The height of the cape is less than 25 m. The moraine material on the cape ranges in size from sand to boulders with diameters up to 3 m. The clasts have low sphericities and are angular.

The ubiquitous moraine material supplies the shore with glaciogenic sediments and thus is the main source of sediment to beach development. The beaches are composed of sediments with a bimodal sorting; medium to coarse sand and pebbles up to 3 cm comprise the finer fraction and big pebbles of 5 cm to cobbles of 7 cm comprise the coarser fraction. At some places where beach development was poor, the moraine material constituted the shoreline.

The only landform in the moraine material display is flutes (Figure 29). The flutes are oriented in an east-west direction (Figure 31). The maximum height is approximately 70 cm. A big boulder marked the landward edge of each ridge. The flutes are several metres long and are unbroken for most of their length, only a few cuts through flutes were observed.

Figure 29 Flutes. The crests of the flutes have been marked with orange. One cut through two flutes has been marked with blue. Location of photo is 78°38'45.02"N, 011°07'46.37"E.

Despite the proximity to Søre Buchananisen and its remains, Andeneset displays a different morphosedimentary environment than at Aurtangen (Figure 31). The coastal zones do however have some similarities; all grain sizes are found except from silt and clay, even big boulders up 2 metres in diameter. Bedrock and moraine material are found in bow-shaped formations in the sea at Andeneset too (Figure 31). Yet the differences are evident. The shoreline at Andeneset exhibit a typical beach morphology, with straight crests of the beach ridges and well-rounded clasts. A cross-section made anywhere at Andeneset (Figure 30) would resemble the sketch of a beach deposit (Figure 4) very well. The area is wave dominated such like the northernmost localities. The shoreline consists of well-rounded beach deposits organized in shore-parallel ridges (Figure 30). The ridge crests are below MHT and a distinctive trough is present behind them. The ridges height decreases south- and westwards from Andeneset. The beach deposits are less distinct

and less steeply inclined the farther the distance westwards from Andeneset. Behind the beach ridge and the trough, beach deposits are situated above MHT and flatten inland. The beach deposits are present up to 20 metres inland and flatten away from the sea.

Figure 30 Berm and backshore. The berm creates a shore parallel ridge. The backshore has an erosive edge towards the sea. Photo from Andeneset, 78°37'9.16"N, 011°14'55.82"E.

The biggest clasts that compose the shoreline are found on the beach ridges, and not in the tidal zone. Sorting of grain sizes was observed in the tidal zone. One segment of sand is at the lowermost level and one segment with coarser clasts, sizes up to 6 cm in diameter, compose the topmost section within the tidal zone. This sorting was best developed at Andeneset headland. The clasts that compose the beach ridges have generally higher sphericities and are better rounded than at Aurtangen.

A lagoon is present close to Søre Buchananisen. It is enclosed by poorly sorted and poorly rounded moraine material on all sides except towards the sea where better sorted and rounded sediment forms the border of the lagoon. The opening is at the western end. Several driftwood logs are present around the lagoon, some at the lagoon´s water level and some logs even 1 m above. This lagoon was not present in 1936 (Figure 25, Figure 26) as the whole area was covered with glacier ice at that time. A spit is found ca. 100 m southwest from the opening of the lagoon separated by a bedrock outcrop with thin coverage of moraine material. The spit is connected to the mainland at its northern end.

Descriptions of grains that compose the shoreline at Andeneset and further west towards Søre Buchananisen are given in Table 3, and the position of each location is shown in Figure 10A.

Table 3 Grain descriptions, Andeneset and Brebukta.

Andeneset/ Brebukta				
Beach Deposit	**Min**	**Max**	**R**	**S**
1	Very coarse sand	10 cm	Sub-angular	High
2 – erosive cut				
Topmost 40 cm	Coarse sand	11 cm	Rounded	High
Middle 20 cm	Coarse sand	8 cm	Rounded	High
Bottom 40 cm	Coarse sand	7 cm	Rounded	High
3	Gravel	25 cm	Sub-angular	High
4	Coarse sand	12 cm	Angular	Medium

Following the shore southwards to Peter Winterbukta, the coastline experiences a gradual transition from unconsolidated beach deposits arranged in ridges to bedrock cliffs with a narrow strip of beach deposits between the bedrock and the sea.

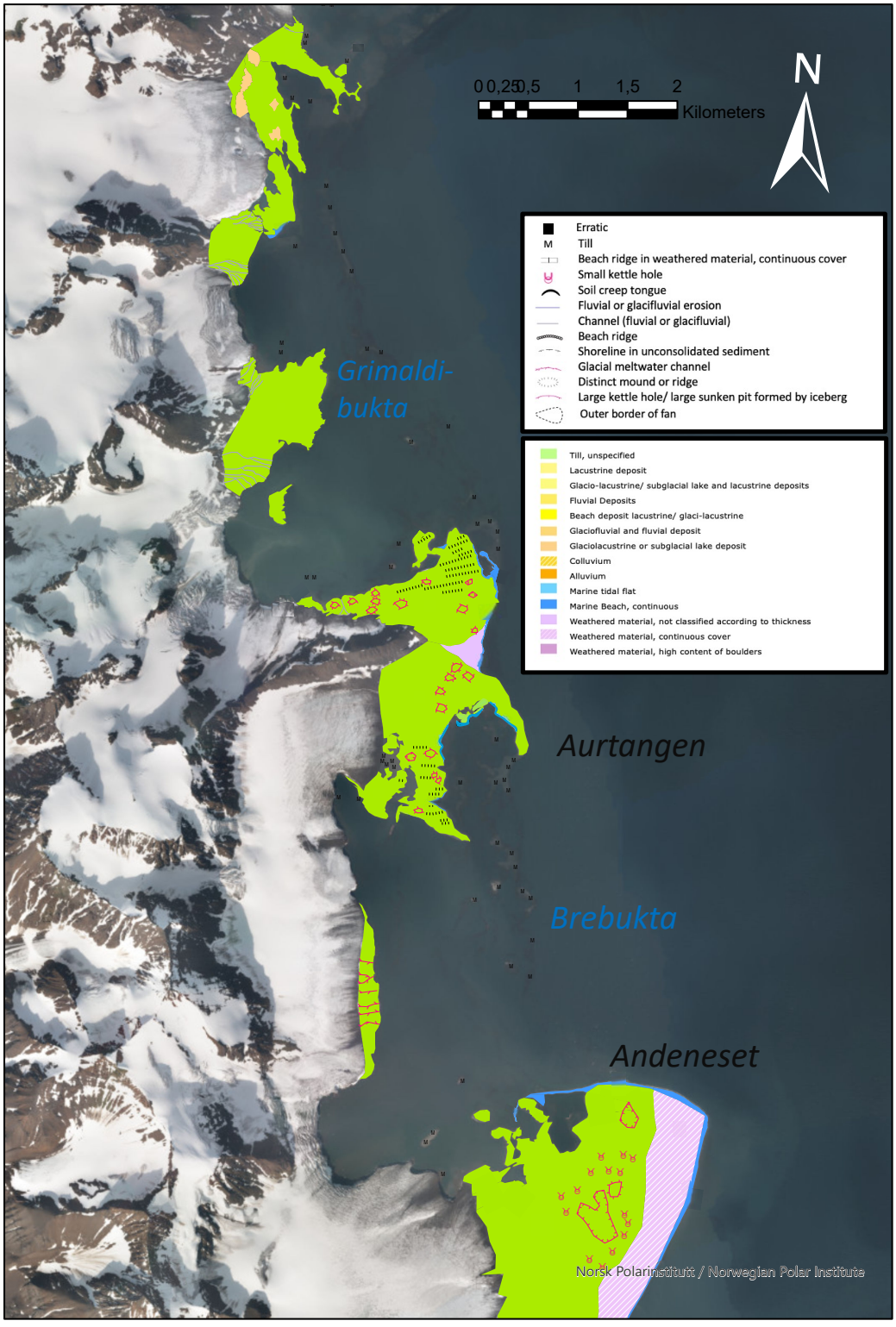

Figure 31 Geomorphological and surficial sedimentological map (Quaternary map) over the middle localities. Interpolation of Grimaldibukta has been made by correlating own observations at Aurtangen and Andeneset with satellite images. Background satellite image courtesy of NPI.

5.3 Alluvium and Colluvium

Figure 32 Map showing the southernmost localities. Map courtesy of NPI.

The shoreline at the southernmost locations of the study sites (Figure 32) is influenced by several processes, however not as much by glacial processes, and thus the depositional features are diverse. The hinterland consists of coastal lowlands and mountains. The mountains have little glacial coverage compared to 1936, but the scope of moraine material is still extensive.

Several waterways that drain the area at Sessflya are small rivers or streams that start up in the mountainside, or from the glaciers or moraines. Two distinct rivers that collect smaller streams are east of Krokodillen and Peter Winterbukta (Figure 32). The sediments brought to the sea are moved away by waves, and no deltas were observed at either of those river mouths. Some material had piled up at the river mouth in Peter Winterbukta between the outcrops of bedrock.

Between Peter Winterbukta and Reinhardpynten the shoreline mostly consists of bedrock cliffs with beach deposits in front. The beach deposits are visible over MHT where it is shallow enough. Where no beach deposits are found in front of the cliffs, the fair-weather waves hit directly onto the cliffs. One lagoon, Marchaislaguna, is present along the shoreline. Beach deposits form the seaside border are found in three distinct ridges, and no opening was observed. The maximum total width of the beach deposits is 50 m. There is a gentle slope from the highest ridge towards the lagoon. Logs are present on the highest ridge only. Seaweed is present on the lowermost ridge only. No rivers or streams access the sea along the shoreline from Reinhardpynten to Marchaislaguna.

The cliffs along the shoreline range in height from 1-3 m and are covered with weathered rocks and dense vegetation. They undulate along the shoreline (Figure 33) and beach deposits are laterally confined by bedrock cliffs. The seaward-facing side of the cliffs is partly covered with scree. The coastline is exposed to waves coming both from the north and the south. The surface of the cliffs had small craters on the edge towards the sea, and one big crater where the ground had collapsed approximately 2.5 m down, down to MHT, was observed next to Reinhardpynten headland (Figure 34). Reinhardpynten seen in the background of Figure 34 is separated from the mainland by a one-metre-wide crack where sea water flows through.

Figure 33 Curving coastline. Beach deposits are between bedrock cliffs. Location of photo: Reinhardpynten, 78°33'37.44"N, 011°17'48.10"E.

Figure 34 Ground collapse. Reinhardpynten is behind the person. Location of photo is 78°33'31.59"N, 011°18'7.73"E.

A description of the grains that compose the shoreline at Sessflya is given in Table 4, and the position of each location is shown in Figure 10B.

Table 4 Grain Descriptions, Sessflya.

Sessflya				
Beach Deposit	**Min**	**Max**	**R**	**S**
1 **Lowermost beach deposit north of Reinhardpynten**	Coarse sand	45 cm	Angular	Low
2	Coarse sand	40 cm	Angular	Medium
3 **Highest ridge** **Middle ridge** **Lowermost ridge**	 Coarse sand Coarse sand Coarse sand	 40 cm 12 cm 15 cm	 Angular Angular Sub-angular	 Low Low Medium
4	1 cm	22 cm	Angular	Medium

The bedrock at location 1 in Table 4 consists of dark shales which can be seen in the cliff in Figure 33. These shales are brittle and generate beach sediments with very low sphericities. North of the headland, at location 2, the sphericity increases slightly and the

type of bedrock changes. Overall, the sphericity and roundness of the clasts composing the beach deposits at Reinhardpynten and Sessflya have low values.

Location 3 is in front of Marchaislaguna, and each beach ridge has been described in Table 4. The highest ridge is approximately 1.5 m above MHT and located 15 m inland from the high-tide swash-mark. The middle ridge is approximately 0.9 m above MHT and located 8 m inland from the high-tide swash-mark and contains erosive edges on the seaside. The lowermost ridge is at the MHT.

Location 4 is at the opening of the braided river east of Krokodillen. The material brought to the sea by the river has been reworked by waves and redeposited and accumulated between two pronounced bedrock outcrops. The author experienced a steep sea floor as she took a swim at this location.

Figure 35 Selvågen. A braided river (marked with yellow) and an alluvial fan (marked with orange) enter the sea, a tidal flat (marked with light blue) is present in front of the river and the fan, and a spit (marked with dark blue) can be seen in the foremost part of the photo. Photo courtesy of Dallmann, NPI.

Selvågen is an approximately 3 km long bay that lies in an ENE – WSW direction (Figure 32, Figure 35). The coastal area was free of ice in 1936 according to aerial photos (NPI). The area that encompasses Selvågen is diverse, rivers run through incised valleys, melt-water rivers originate from small glaciers, mountains with steep slopes surround the bay, and cliffs are found by the sea. The sediments brought to the shore are reworked by different processes such as waves, ocean currents and tides into landforms such as beach ridges and spits which are observed along the coastline.

The catchment area of the rivers that enter Selvågen is approximately 30 km^2. Alluvial and colluvial fans and slope processes, in addition to rivers, contribute with substantial amounts of sediment to the shore (Figure 38). The origin of these sediments is from the mountains directly and from moraine material. Some of the rivers are meltwater rivers that originate from glaciers, but these rivers are small. The longest river runs through Scotiadalen and is 4.5 km long. In the upper part of the river, the channel is partly confined by bedrock and incised in the valley, while near the river mouth it broadens into a braided channel river (marked with yellow on Figure 35).

The former extent of Doddsbreen has left a great end moraine in the landscape which glacial meltwater has cut through. This meltwater gave rise to an alluvial fan on the southern side of the bay (marked with orange on Figure 35).

A spit is present on the northern side of the bay (marked with dark blue on Figure 35) (Figure 38). Incoming waves break with an angle along this depositional feature. The spit consists of sediments that are poorly rounded. Close to the tip of the spit, more seaweed was found on the seaward side and more moss was present on the inner side than what was the case for the parts of the spits closer to the mainland. The sediments decrease in size towards the spit tip (Table 5). The tip of the spit is divided in three parts, where the innermost tip consists of the coarsest material relative to the other tips. The finer fraction composes a greater part of the bulk sediments of the outermost tip. A cross section of the surface of the spit showed a sequence of fine – coarser – fine sediments when moving from the sea to the top of the spit and then down to the environment on the inside of the spit. A tidal channel is in front of these spit tips, between the spit tips and the marine deposits in front of one of the colluvial fans (Figure 38).

On the mainland side of the tidal channel, a colluvial fan enters the sea and creates a small fan delta. Both sides of the colluvial fan are confined by bedrock. The seaward border of the delta is where the tidal channel outside the spit tips flows. The colluvial fan has inactive parts with dense vegetation cover that is approximately 3 cm thick, inactive parts where the channels are dry but no vegetation is present, and active parts where the channels are wet.

Following the coastline further into the innermost part of the bay, slope processes are observed (Figure 3, Figure 38). Rocks have eroded from the cliffs and fallen onto the beach. The debris consists of angular rocks with diameters up to 20 cm (Figure 3). Other than that, gelifluction had occurred. The top layer of the weathered ground cover and

vegetation had moved downslope. The fracture edge at the back of the sliding masses is approximately 20 cm high. This is marked with the sign for soil creep tongue on Figure 38.

A big tidal flat covers the innermost part of the bay in a crescentic shape from north to south (Figure 7, marked with light blue on Figure 35 and Figure 38). The processes which contribute with sediments to the tidal flat are alluvial, colluvial and fluvial processes (Figure 38). The river mouth is approximately 630 m at its widest at the coastline. Fan shaped deposits that terminate at or near the sea (Figure 38) contribute with sediment supply to the tidal flat. Three colluvial fans are present north of the braided river, where the northernmost has a higher gradient than the others. The last fan shaped deposit consists of alluvium. This fan originates from the end moraine of Doddsbreen and merges with the braided river. Glacial meltwater runs through the alluvial fan (Figure 38).

Beach deposits and a spit are also present on the southern side of Selvågen. This spit is too small to be visible on the geomorphological map (Figure 38). The beaches on the southern side of Selvågen have several beach ridges (Figure 36), which is not the case for the northern side of the bay nor at Andeneset. The ridges are composed of coarser material on top of the ridges than at the ridge faces (Figure 36). The beaches on the southern side consist of generally finer material compared to the beach deposits on opposite side of the bay (Table 5). At some sections along the southern side of the bay, 2 metres high bedrock cliffs compose the shoreline. The closer the beach is to an exposed section of bedrock, the coarser the beach deposit is. The beaches are confined between pronounced bedrock cliffs.

Figure 36 Beach deposits at Dawespynten. Three distinct ridges are seen in front of the backshore, indicated with yellow. The dried seaweed seen in front is above MHT.

The bedrock cliffs at Reinhardpynten continue along the shoreline on the northern side of Selvågen for approximately 1 km. Narrow beaches are situated in front of these cliffs (Figure 38) and consist of sub-angular to angular clasts (Figure 37). The cliffs range in height from 1 to 4 m and the beach deposits are coarse clastic with sizes up to more than 90 cm in length (Table 5, Figure 37). At some sections along the cliffs, few or no beach deposits are present. A description of the grains that compose the shoreline at certain sections in Selvågen is given in Table 5, and the position of each location is shown in Figure 10C.

Figure 37 Coarse clastic beach. Biggest clasts are 95 cm in diameter. From the northern side of Selvågen (location 1 in Table 5), 78°33'25.6"N, 11°16'42.3"E. Photo by Ronja Arum.

Table 5 Grain descriptions, Selvågen.

Selvågen				
Location	**Min**	**Max**	**R**	**S**
1	Coarse sand	95 cm	Very angular	Low
2	Coarse sand	60 cm	Angular	Low
3	Coarse sand	25 cm	Angular	Low
4	Coarse sand	15 cm	Angular	Low
5	Coarse sand	10 cm	Angular	Low
6 - spit				
Innermost tip	Coarse sand	5 cm	Angular	Medium
Midst tip	Coarse sand	5 cm	Angular	Medium
Outermost tip	Coarse sand	3 cm	Angular	Low
7	Coarse sand	3 cm	Very angular	Low
8	Coarse sand	3 cm	Angular	Medium
9	Silty sand	4 cm	Sub-angular	Medium
10	Medium sand	19 cm	Sub-angular	Medium
11	Fine sand	9 cm	Sub-angular	High

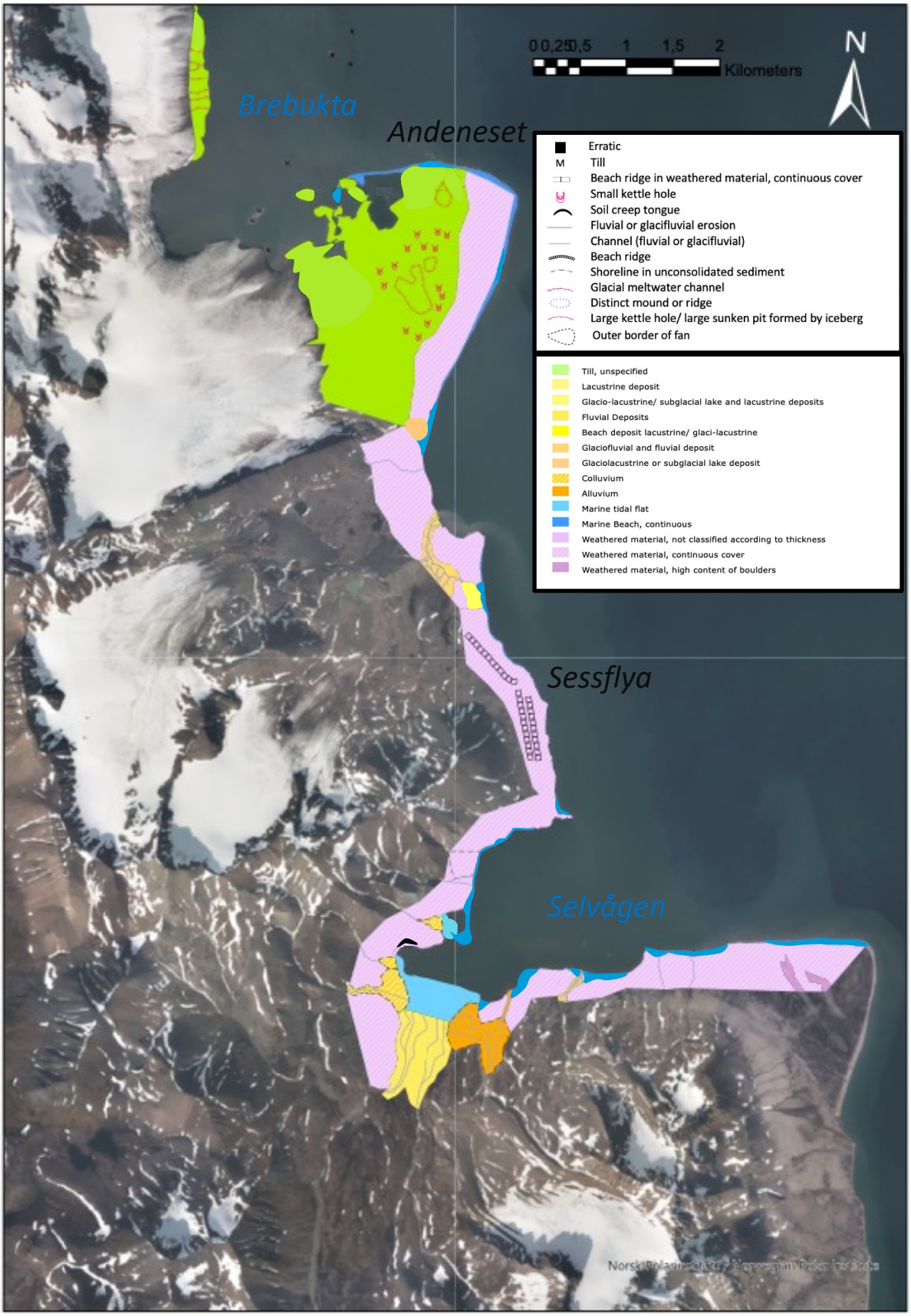

Figure 38 Geomorphological and surficial sedimentological map (Quaternary map) over the southernmost localities. Background satellite image courtesy of NPI.

5.4 Results from 14C-sampling

Table 6 14C Ages of samples

Object		Position			14C Ages (rounded)
1	Shell fragments	Murraypynten	78°43'58.68"N	011°09'0.42"E	10,490 ± 55 BP
2	Log	Andeneset	78°37'1.33"N	011°15'30.98"E	125 ± 15 BP
3	Whale bone	Richardlaguna	78°46'23.82"N	011°02'21.35"E	1515 ± 15 BP
4	Log	Murraypynten	78°43'31.83"N	011°08'50.30"E	85 ± 15 BP
5	Log	Richardlaguna	78°46'14.42"N	011°04'10.29"E	100 ± 20 BP
6	Whale bone	South of Fuhrmeister-stranda	78°44'36.60"N	011°09'13.83"E	750 ± 15 BP
7	Log	Richardlaguna	78°49'11.71"N	010°59'7.18"E	170 +15 BP

The purpose of dating logs, whale bones and shell fragments is to get information about ages of and thus be able to tell the landform evolution.

6 DISCUSSION

The sections that have been investigated along the north-eastern coast of Prins Karls Forland show high geomorphological variability. The main similarity of the study sites is the proximity to glacial deposits and processes, both spatially and temporally. Of the study sites, Selvågen and the barrier complex in front of Richardlaguna are the two locations that have been deglaciated for the longest time interval. Brebukta was covered with glaciers in 1936 and is still being deglaciated. The study sites are controlled locally by different processes. The dominating processes controlling the coastal development at the north-eastern coastline of PKF will be described below.

6.1 COASTAL DEVELOPMENT IN GLACIATED VS. NON-GLACIATED REGIONS

Several factors contribute to coastal development in areas that are still glaciated or have recently been deglaciated. In recently deglaciated coastal areas the sediment availability is higher than in areas which have been free of ice for a longer time interval. Unconsolidated glaciogenic material covers the coastal areas, both on land and in the nearshore area and consequently the sediment supply is abundant. The sediments that compose the beaches are angular and have low sphericities, especially when compared to sediment that compose the shoreline at wave exposed sites.

There is a correlation between proximity to glacier, spatially and temporally, and sediment size. Though the shoreline morphology at Andeneset and Dawespynten is alike, both locations have the same orientation and exposure to waves, and the bedrock at the two headlands consists of clastic sedimentary rocks (NPI), the beach ridges at Dawespynten have a bulk composition (Table 5) that is finer than at Andeneset. Under the same wave conditions, the shoreline that is located closest to glaciers and glaciogenic material will develop beaches consisting of coarser material compared to shorelines with a greater distance to glaciers, temporally and spatially.

At coastal sites that were glaciated 85 years ago, single boulders deposited by the glacier play a major role in how beaches develop. The glaciogenic boulders control beach development by influencing the flow pattern of tidal currents and dampen incoming waves. The beaches in these areas are modestly developed, as the paraglacial sedimentation has not had the time to develop beaches to a great extent. At most of the

coastal sites where deglaciation has taken place during the last 85 years, tidal processes play a bigger role in redistribution of sediment and thus shaping the shoreline than at coastal sites where wave action dominates.

6.2 THE NORTHERNMOST LOCALITIES

The coarse gravel beaches at the northernmost localities all belong to the same dynamic system. The same type of modern beach deposit with respect to size, roundness, sphericity, continues southwards from Heemskerckneset to Murraypynten. The barrier complex, Fuhrmeisterstranda and Murraypynten exhibit geomorphology and evolution dominated by wave processes.

6.2.1 The Barrier Complex

The barrier complex can be defined based on the number of openings/ tidal inlets that cut through (Otvos, 2012). The barrier complex has alternated between having one or two mainland attached barriers, and one or no barrier islands between. In 1936 and 2021 there was one barrier island between the parts attached to the mainland, while in 2008 there was no barrier island present.

Two propositions for the evolution and origin of the clasts that form the barrier complex are discussed here, following the suggestion of Bluck (2011): originating from glacial deposits or from erosion of nearby cliffs.

6.2.1.1 Proposition 1: barrier originating from glacial deposits

The whole barrier complex can be interpreted as a postglacial end moraine deposit, established after a thermal minimum in the Pleistocene when glaciers reached their largest extent on Svalbard.

The end moraine was left at the same time as the glacier that covered PKF was detached from the Spitsbergen ice sheet in the late Pleistocene sometime after 13,800 years BP (Butschek et al., 2019; Landvik et al., 2005). As the temperatures continued to increase, the glacial cover of PKF melted into several smaller glaciers that filled the valleys behind Richardlaguna until the glaciers had melted completely and left the whole island fully deglaciated during Early and Middle Holocene (Farnsworth et al., 2020).

6.2.1.1.1 Sediment source

The presence of finer material such as sand, and less well-rounded clasts found in the erosive cuts within the barrier ridges (Figure 20) could indicate that the whole barrier

complex is not exclusively a beach deposit created entirely by waves, but could originate from an end moraine. The erratic observed on the landwards side at the southern end of the barrier complex is of glaciogenic origin. Sediment in the barrier complex could have been recycled from a proglacial end moraine by wave action into amalgamated spits.

The presence of finer material within the barrier complex can also be explained by weathering of rocks. Thermal abrasion (Are, 1988) and/or frost wedging are the processes than can be held responsible for the creation of smaller grains as waves constantly work in the barrier and the temperatures is often below zero degrees.

6.2.1.1.2 Spit amalgamation

The comprehensive amalgamation of spits explains why the barrier complex consists of curved ridges with distinct troughs between them. The point of origin of a new spit is where the former spit curves. As this is repeated successively the clear and straight shore-parallel ridges are formed. Lateral migration of spits is the result of deposition (Oertel, 1985). This lateral migration has resulted in the water-filled ponds (small lagoons) within the barrier on the northern part.

6.2.1.1.3 Wave reworking

Incoming waves, both swells and wind generated waves across Forlandsundet, have reworked the ridges of the barrier complex at several sections as the openings have changed position over time (Figure 39). This is the case for the northernmost ridges in the southern part of the barrier complex (Figure 16). The southern ridges curve differently than the ridges in the middle and northern parts, but this appearance is due to erosive forces working through the tidal inlet as Oertel (1985) and Tribe and Kennedy (2010) stated.

6.2.1.1.4 Tidal influence

The tidal prism of Richardlaguna was strongly restricted when only one inlet was present in 2008. In the course of time the barrier could not withstand the tidal influence and accordingly a new tidal inlet appeared. This change is most likely to have occurred during a storm event as the whole barrier complex is then vulnerable to great forces by tidal influence, waves, winds and thus longshore currents. The inlets play a role in long-term evolution of the barrier complex allowing tidal currents together with wind generated waves from within Richardlaguna to erode the landward border of the barrier complex and thus created the steep edge towards the lagoon. Migration of tidal inlets has occurred downdrift as a result of spits that have been amalgamated onto the barrier and

tidal currents that have kept the inlet open (Figure 39). When tidal currents cannot overcome the spit accretion, the inlets can be closed off, which occurred with the southern inlet of the barrier complex from 1936 (not visible on Figure 39).

Figure 39 Position of the openings and the barrier itself from 1936 to 2021. The red lines indicate the position in 2021, the blue lines 2008 and the dashed line 1936. Where the border of 2008 overlaps with the border from 2021, the blue lines have been made transparent, so both are visible. Background satellite image courtesy of NPI.

6.2.1.1.5 Barrier complex migration

The migration towards land of the whole barrier complex is most evident in the middle part in Figure 39. As Figure 39 evidently shows, the position in 1936 which is indicated with a black dashed line is further towards the east than in 2008 (indicated with blue lines) and in 2021 (indicated with red lines). What is interesting is the middle section of the barrier where it has migrated outwards from 2008 to 2021 (Figure 39). During the same time interval, the barrier developed a new tidal inlet which aided in controlling morphological evolution of the barrier.

Although the barrier complex has experienced total net accumulation (Figure 40), there are sections along the seaside on the northern part of the complex that have experienced

local erosion (Figure 39). In comparison to the north where migration has occurred towards land, the southern part of the barrier complex has prograded towards the sea (Figure 16). The southern section has experienced little local erosion if any. This implies that sediment supply to the barrier is sufficient and that the productive processes work sufficiently.

The primary mechanism of migration is due to roll-over by storm-wave activity which redistributes sediment over the barrier crest into wash-over lobes (Masselink et al., 2011c; Orford et al., 1991a). Numerous wash-over lobes were observed along the back-barrier for the whole length and the satellite images show clear lobe structures on the back-barrier (e.g., Figure 16). The wash-over lobes observed during the fieldwork have buried older wash-over lobes and will themselves likely be buried by newer wash-over deposits as storms strike. This continues as storms hit the shoreline and leads to the sediment that was once on the back-barrier will emerge at the shoreline and new storms will access it to create new wash-over lobes.

6.2.1.2 Proposition 2: barrier originating from eroded cliff material

The second proposition for the development of the barrier complex is based on swell/ wave action and sediment supply from the upstream headland. The swells hit PKF from the northernmost point, Fuglehuken, to Heemskerckneset and follow the coast south and eastwards by refraction. The refraction of swells and waves can be interpreted as the main cause of clast transport and hence the main cause of coarse clastic barrier and beach evolution from Heemskerckneset to Murraypynten.

6.2.1.2.1 Sediment source

The abrupt change in the coastline at Heemskerckneset is the initial outset for sediment deposition that has created the barrier complex. The sediment comes from erosion of alongshore areas (Figure 40). This type of source was also described by Forbes et al. (1995b) who stated that most paraglacial coasts are reliant on coastal erosion for the sediment supply. Evolution of barrier systems that are built by accumulation of eroded alongshore material can occur under relative sea-level falls (Forbes et al., 1995b) which Svalbard experiences today. Measurements from behind Richardlaguna shows yearly uplift of 4.3 mm (NRK, 2022).

6.2.1.2.2 Formation and evolution of the complex

The barrier complex can be interpreted as a drift alignment constructed with sufficient sediment supply. An illustration of the barrier complex evolution due to this mechanism

is shown in Figure 40. In this scenario, the complex initially started as a spit (Figure 40B) that gradually advanced in the down-drift direction by amalgamation of deposits that formed spits and berms and thereby beach ridges (Figure 40C). This stage coincides with the earliest stage of evolution of a drift alignment of Forbes et al. (1995b). The deposits subsequently accreted in crescentic formations at the end of the spit and evolved into a barrier (Figure 40D). The accretion of spits into a barrier can have occurred over a relatively short amount of time if the bathymetric conditions were favourable according to Forbes et al. (1995b). If the sediment supply had been insufficient the barrier formation would have been segmented (Forbes et al., 1995b). Sediment supply has overall remained sufficient as erosion of bedrock cliff in the up-drift direction has prevailed and the longshore drift been strong enough to transport the eroded clasts.

As storms have hit the barrier, the stable structures broke down, sediment was eroded, redistributed and mixed, and tidal inlets evolved and broke through the barrier (Figure 40E). A newly hit barrier is more susceptible to changes by new storms. During longer phases of no storms or small storms, the barrier has time to restabilize as longshore drift prevails and the sediment supply continue (Forbes et al., 1995a). Restabilizing of the barrier and repeated spit accretion persist until a new storm hits and sediment is once more eroded, redistributed and mixed and new tidal inlets emerge (Figure 40F).

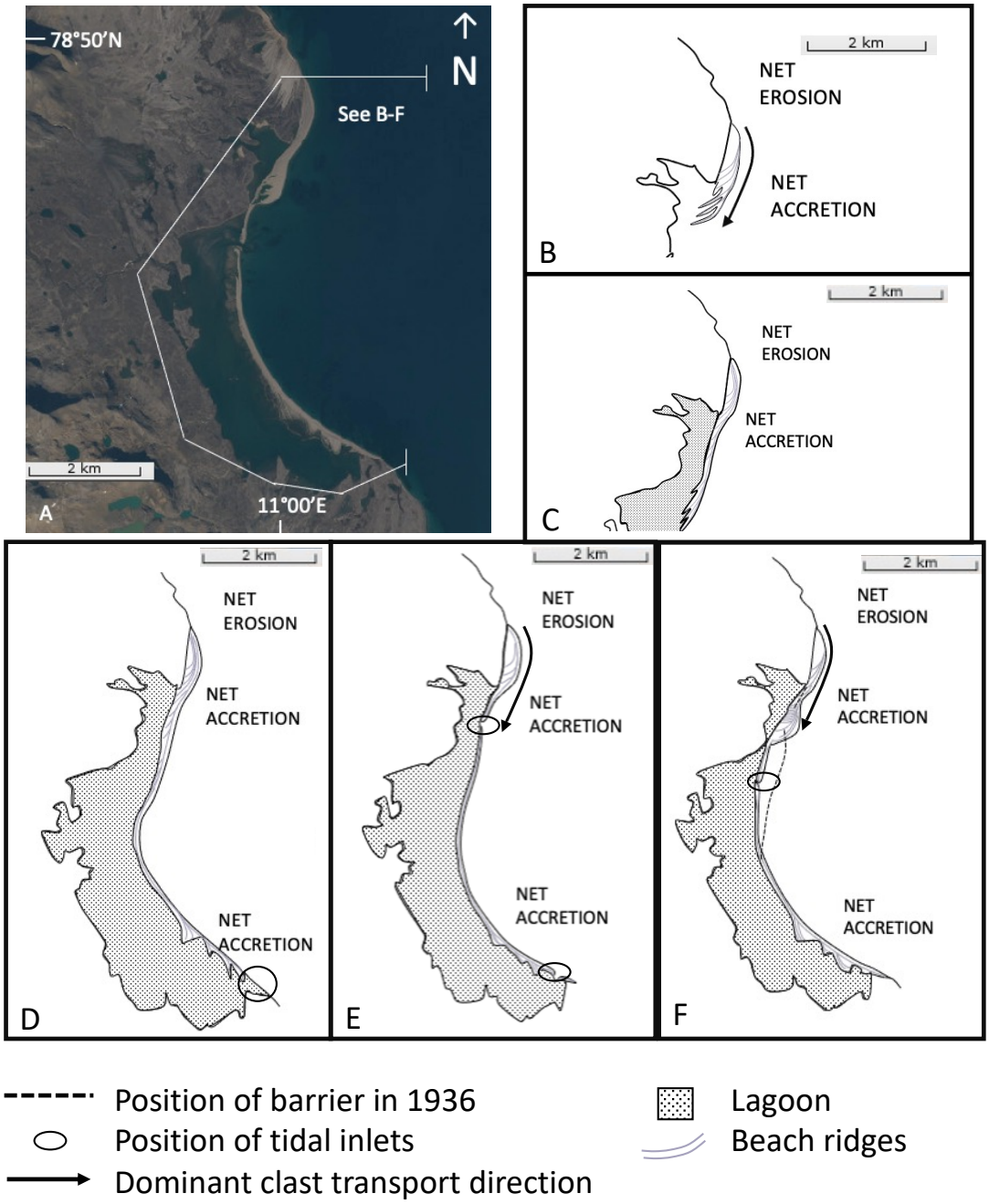

Figure 40 Evolution of the coarse clastic barrier complex in front of Richardlaguna. The barrier is evolving by longshore drift. A: Satellite image over the barrier complex from 2008. Background satellite image courtesy of NPI. B: The initial spit that developed into a barrier. C: Spit advances down-drift as beach deposits are amalgamated onto it. D: Richardlaguna is nearly enclosed by the barrier. E: Two openings/ tidal inlets dissect the barrier. F: Only one opening as the southernmost one from E has been closed by beach deposits.

The first and second proposition for barrier evolution can both be correct as the sediment source can come from both an end moraine and erosion of nearby cliffs. Regardless of sediment source, the processes that have reworked the sediment is the same for both propositions.

6.2.2 Fuhrmeisterstranda and Murraypynten

Wave action and longshore drift have not only formed the barrier complex, but also the beach deposits along Fuhrmeisterstranda and Murraypynten.

6.2.2.1 Erosion of the bedrock cliffs of Fuhrmeisterstranda

Wave erosion and undercutting (Atkinson, 2005; Dickson et al., 2009) are limited along the bedrock cliffs of Fuhrmeisterstranda due to protection by the beach deposits. The erosive edges of the cliffs are either due to wave erosion when the sea level was higher (1000 years BP, 5000 years BP or 9000 years BP and older (Forman, 1990)) or due to frost wedging/ -shattering, or a combination of the two.

6.2.2.2 Relative ages of the beach ridges

The innermost beach ridges are obviously older, shown by the amount of vegetation present. The different orientation (Figure 22) of these ridges compared to the outer ridges suggests that there has been a shift in dominant incoming wave direction. The time of deposition of the older ridges can be up to 9000 years BP as the sea level has fluctuated ca. 4 m around the present day sea-level at PKF according to (Forman, 1990).

6.2.2.3 Murraytjørnene

The presence of shell fragments at Murraytjørnene indicates that marine processes have worked at the coastal section behind today´s modern beach deposits. At the time the shells were created (10,492 ±54 years BP), the sea level was 30 metres above present day sea-level (Forman, 1990) and the glaciers on PKF melted (Farnsworth et al., 2020). The Murraytjørnene lakes are thus a result of glacial processes in the Pleistocene and tidal processes. The modern beach deposits prevent contact between the lakes and the sea.

6.2.2.4 West of Murraypynten

The recent retreat of Murraybreen west of Murraypynten, northern part of Grimaldibukta, has left extensive amounts of glaciogenic deposits. This coastal section is not dominated by wave impact but by paraglacial processes such as in Brebukta (see below).

6.3 THE MIDDLE LOCALITIES; AURTANGEN, BREBUKTA AND ANDENESET

Paraglacial sedimentation, the rearranging and sorting of glaciogenic sediments (Church & Ryder, 1972), is the key process controlling shoreline evolution in Brebukta based on geomorphological features observed during fieldwork. Westwards from Aurtangen stretches Brebukta, where a combination of glaciogenic material, micro- to marginal meso-tidal range and energetic waves allow gravel-dominated geomorphological features to develop. The cover of glaciogenic deposits varies in thickness and in morphology. The importance of the flutes is observed in their ability to provide sediment supply to the shoreline.

6.3.1 Aurtangen

Much of the development of the gravel-dominated beaches in Aurtangen arises from erosion of glaciogenic material, including from the outer-most flutes, by storm-generated swells and waves. Wave attack against flutes or other glaciogenic material releases sediment which functions as a source for beach formation. Wave action together with glacial runoff by melt water and rain constantly remove glaciogenic material. Beach development continues as sediment supply persists. Storm-generated swells and waves from the south and south-east are especially effective along the south-facing headland area. Incoming swells and waves are refracted and directed by the profoundly irregular bathymetry and by glaciogenic sediment in the sea. This together with greater waves under storm events creates local longshore currents that transport sediment at the shoreline and in the nearshore area.

The wash-over lobes found at the bay at Aurtangen are products of storms waves at a wave dominated coast. So are the erosive edges and logs found in and on the beach deposits. The drainage channels that cut through the wash-over lobes assist the shoreline in developing from a wave-dominated to a more tidal-dominated environment. Tidal currents can erode in areas of the shore where swells and waves did not have the power to erode due to dampening by bathymetric conditions and the glaciogenic boulders.

Andeneset headland is not subject to paraglacial sedimentation but is dominated by wave processes.

Following the shore westwards from Andeneset, the beach deposits are less steeply inclined and consist of finer deposits. The spit that has developed west of Andeneset

headland after or at the same time as the deglaciation occurred, signal the presence of longshore currents. Incoming waves, both from the north and from the south, are reduced in size and energy by the time they reach the innermost part of Brebukta due to the boulders present in the sea. This indicates lower wave impact and a greater control by currents and longshore drift at the inner sections of Brebukta. This is supported by the grain descriptions given in Table 3: the clasts at the headland have a higher degree of roundness which is a result of wave action, compared to the clasts at the shoreline that are located closer to the front of Søre Buchananisen where glaciogenic sediment dominates the shore and the wave impact is lower.

6.4 THE SOUTHERNMOST LOCALITIES, SESSFLYA AND SELVÅGEN

The cliffs along the coast at Sessflya and the outer parts of Selvågen are exposed to swells/ waves. This implies that the coastal sections at Sessflya and outer parts of Selvågen is prone to erosion by thermal and mechanical energy from the sea. The beaches situated in front of the cliffs protect the cliffs to some extent from thermal abrasion.

6.4.1 Grain size distribution

Based on maximum grain size, the spit on the northern side of Selvågen shows lateral sorting extent (location 3, 4, 5, and 6 in Table 5). Whether this is due to wave action primarily, longshore current or tidal influence is difficult to determine. The shore at the inner parts of Selvågen consists of generally finer material (location 7, 8, and 9 in Table 5, Figure 10) than the outer parts of Selvågen. This indicates less wave impact as the waves would have eroded the finest grains.

6.4.2 Sediment source processes

Frost weathering/ -shattering together with gelifluction produce deposits of (nearly all) grain sizes and thus contribute to coastal sediment with a major gravel component. Surface areas can absorb solar radiation and be warmed by air. This gives warmer temperatures locally and less reflection of solar radiation. The recently deglaciated material can be eroded and brough to the sea where marine processes such as waves and longshore currents can redistribute the sediments.

6.4.3 Dominant processes at Selvågen.

Based on field observations, the shoreline morphology at the inner parts of Selvågen is not wave dominated but rather tidal-, alluvial-, colluvial-, delta- and slope process dominated.

6.5 14C-DATING

The purpose of 14C-sampling was to help dating the ages of the landforms, however, the then samples were from a much younger age than expected and thus did not give any clear indications regarding landform evolution, except for the shell fragments.

6.6 THE KEY PHYSICAL PROCESSES

The key physical processes that dominate and/ or influence the coastal evolution are summed up in Figure 41. Although the studied coastline is not located at the open coast, the sites are exposed to large swells and waves. The swells and waves, along with wind, generate longshore currents. Waves together with longshore currents erode, transport and deposit sediment and thus control the coastal morphology. The evolution of shoreline geomorphology at the north-eastern coastline of PKF is primarily wave dominated, with wave direction coming from the north (Figure 41). Because of the shallow point between Sarstangen and Murraypynten (maximum depth 3 metres), the incoming swells and waves from the north are dampened to some extent on their way south through the sound and incoming swells and waves from the south are dampened on their way north. Accordingly, Forlandsundet functions as two basins with respect to the dominant longshore drift pattern. On the west side of Forlandsundet the dominant longshore drift direction is southwards (Figure 41). This is supported by the geomorphology of the landforms observed during fieldwork. On the east side of Forlandsundet, the longshore drift direction is northwards in the southern part and southwards in the northern part. This longshore drift pattern is responsible for the formation of Sarstangen (Figure 41).

Local and specific processes overprint the dominant process, and thus control the morphology, in inner parts of bays where wave action is less powerful. The shore morphology of the inner parts of Selvågen is not wave dominated as the topography protects the bay from high energetic waves, but is rather controlled by tidal-, alluvial-colluvial, delta-, and slope processes. The shore morphology at Aurtangen and Brebukta, both sites which have recently been deglaciated, is controlled by the main processes which are directed and focused by the bathymetric conditions and the presence of glaciogenic material in the sea.

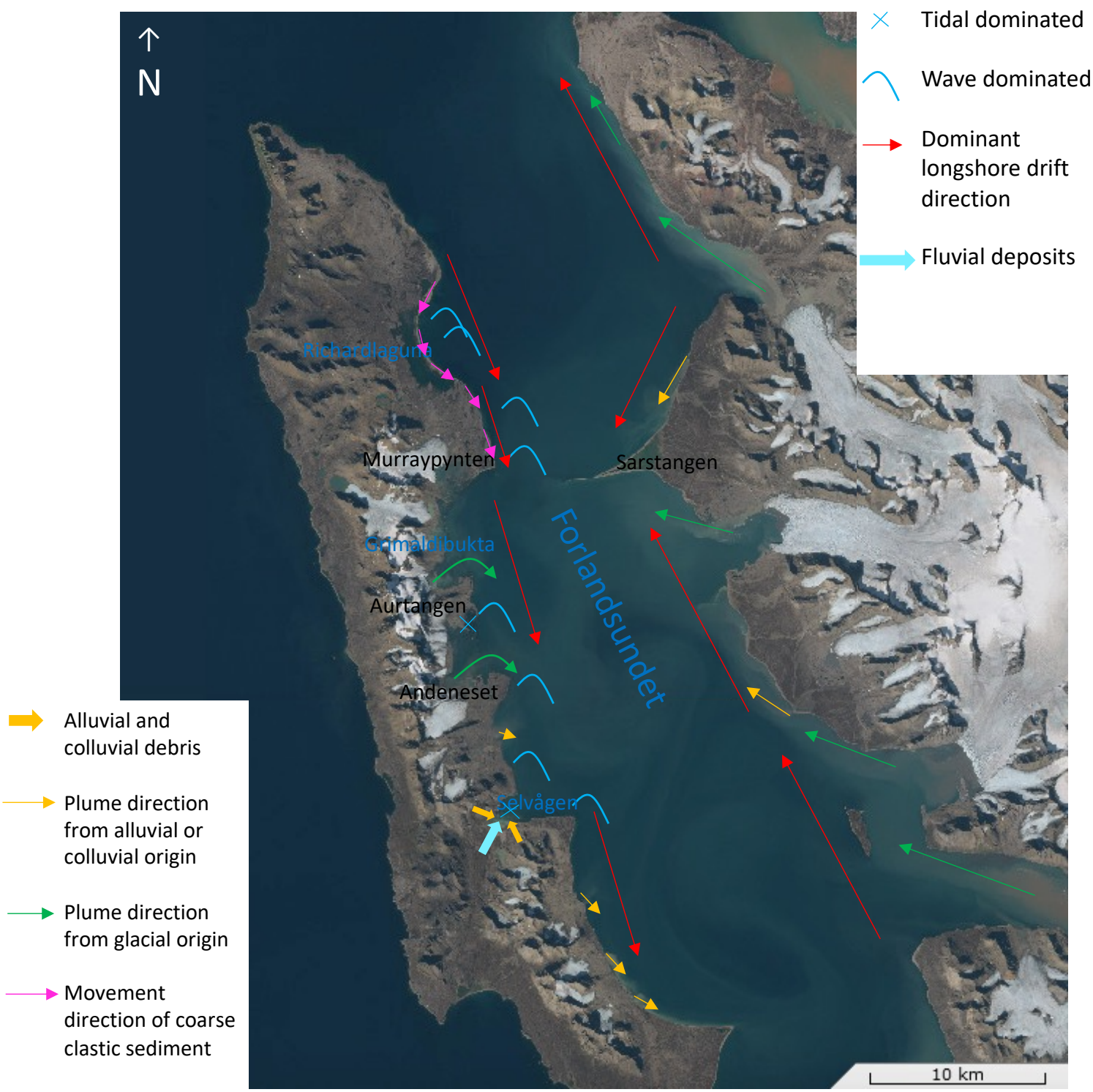

Figure 41 Main processes that control coastal development at the north-eastern coastline of Prins Karls Forland. The shallow area between Sarstangen and Murraypynten divides Forlandsundet into two basins with respect to longshore drift currents and tidal currents. Background satellite image courtesy of NPI.

6.7 COASTAL PROCESSES OBSERVED IN THE STUDY AREA PROJECTED TO PREDICT FUTURE DEVELOPMENT

As stated by Sollid and Christiansen (2003) the two most important factors for coastal evolution in the Arctic are climate and distance to the ocean. Climate is a broad term comprising many features, all of which are increasing: aerial temperatures (Førland et al., 2011; Hanssen-Bauer et al., 2019), surface temperatures (Sobota & Nowak, 2014), precipitation rates (Førland et al., 2011), ocean temperatures (Smedsrud et al., 2022), and storminess (Atkinson, 2005; Savelieva et al., 2000; Serreze et al., 1993). These climatic features influence coastal evolution in many ways.

The barrier complex will continue its landward migration in the north, but whether the migration is a result of single storm events, a general increase in storm frequency, or a combination of the two (Forbes et al., 1995b) is rather difficult to predict. The increasing storm frequency together with a lack of sea ice during autumn and winter in Forlandsundet facilitate greater wave impact along the coast and thus the migration of the barrier complex towards land is expected to increase further. In the southern part of the barrier complex the migration is expected to continue in its seaward direction. Sediment supply is expected to prevail as wave action and frost wedging/ -shattering will provide material, or even increase as Arctic storminess patterns show an increasing trend.

The recently deglaciated area of Brebukta is expected to have better developed beaches as paraglacial sedimentation continues along with swells/ waves and longshore current to influence the shoreline morphology. The beach development is expected to continue due to a greater runoff caused by increasing precipitation and temperatures (and hence more melt water from the glaciers). Søre Buchananisen is expected to retreat completely and thereby exposing the currently ice-covered shorelines to swells/ waves and longshore currents.

The terrestrial processes in the inner parts of Selvågen are expected to accelerate as the permafrost thaws due to increasing ocean temperatures (Kristensen et al., 2008) and thawing of the permafrost is strongly linked to coastal erosion (Masselink et al., 2011a). The active layer thickness will increase and thereby lead to more active of slope processes. Increased precipitation will give greater runoff, and thereby greater deposits by alluvial, colluvial processes and fluvial processes. As more material is eroded and brought to the sea, the delta and tidal flat will expand and thus the shoreline is expected to prograde.

7 CONCLUSIONS

1. The determination of the key physical process that dominates the coastal evolution of north-eastern Prins Karls Forland is based upon morphological features observed during fieldwork and the study of aerial photos and satellite images. The dominating process is swells/ waves coming from the north. This dominant process is overprinted at Selvågen and Brebukta so that local processes dominate coastal evolution. The barrier complex in front of Richardlaguna and the coarse gravel beaches at Fuhrmeisterstranda and Murraypynten are dominated by wave processes from the north. In Selvågen the numerous slope processes and tides control shoreline development. In Brebukta, paraglacial sedimentation along with tides control shoreline development.
2. Recently deglaciated areas display a different morphology than areas that have been deglaciated for a longer time: the coastal area and/or backshore area is covered with extensive amounts of glaciogenic deposits, the shoreline consists of more angular clasts, the beaches are modestly developed if present at all, and the overall morphology of the shorelines is more irregular.
3. The coastal processes observed in the study area can be used to predict future development in a warming climate. The processes already controlling the coastal evolution is expected to increase in strength/ mass. The barrier complex will continue its landward migration in the north, tidal inlets will be closed off by spit accretion and new inlets will cut through the deposit during storms. Accretion of spit is expected to continue as no indicators of any future decrease in sediment supply has been detected. The paraglacial sedimentation in Brebukta will continue as waves, longshore currents and tides continue to rework the glaciogenic sediment into beach deposits. The slope processes in Selvågen are expected to erode more material from the mountain sides and from the valley which will be brought to the delta and tidal flat. These depositional features are expected to continue prograding.

8 FUTURE WORK

To verify the propositions suggested to explain the origin and evolution of the barrier complex, mineralogy of the clasts composing the barrier can be checked and correlated with the mineralogy of the cliffs at Heemskerckneset and northwards. The core of the barrier can be examined with ground-penetrating radar. Suitable sand grains from within the barrier can be used for luminescence dating if present, however, that was not observed during fieldwork. Shell fragments from the barrier complex, if any are present, can be used to date different parts of the barrier. Shell fragments were not observed within the barrier either. The depth of Richardlaguna could be investigated to get a better understanding of the origin of the barrier complex. A deep lagoon can imply a stillstand of a former glacier over a longer period and thus the creation of a great end moraine, while a shallower lagoon can indicate lagoon formation by glaciofluvial erosion.

Hydrological modelling of longshore currents in Forlandsundet would aid in predicting future development of the coast and shoreline more precisely. Monitoring of the sea-level at PKF would also aid in predicting future coastal development.

14C-dating of biological material from a place where the sea-level has fluctuated should be carried out on objects that are buried. This could aid in determining the ages of landforms.

9 APPENDIX

Legend to the maps provided by NPI

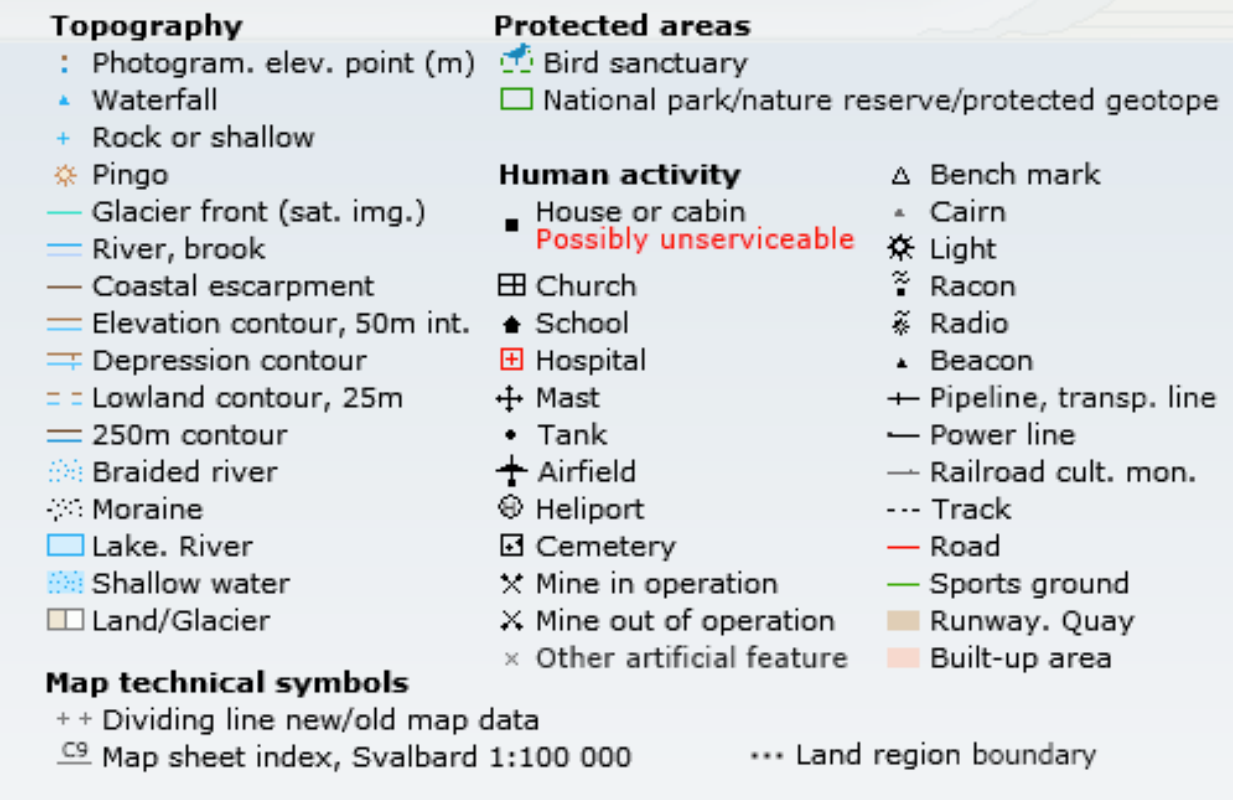

Locations of all photographs taken by the author

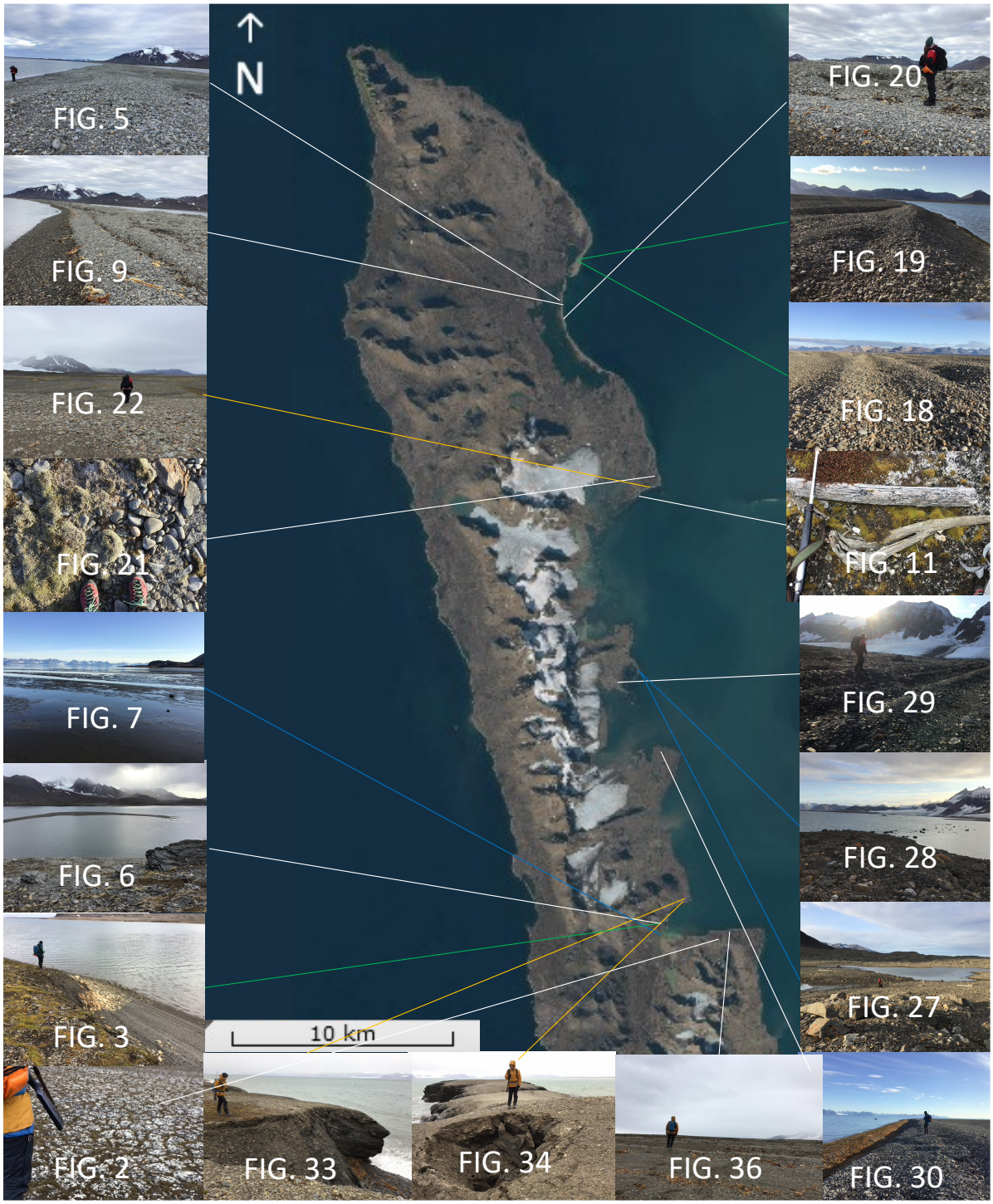

All locations of the photographs taken by the author are indicated with lines. The different colours of the lines have been made to make it easier to see the exact location. Background satellite image courtesy of NPI.

Tracks made along MHT

Tracks are uploaded from Garmin to Google Earth and overlain on satellite images from 2011, not from 2022 as the images say.

From Murraypynten:

From northernmost part of Richardlaguna:

From the northernmost section at the southernmost part of Richardlaguna:

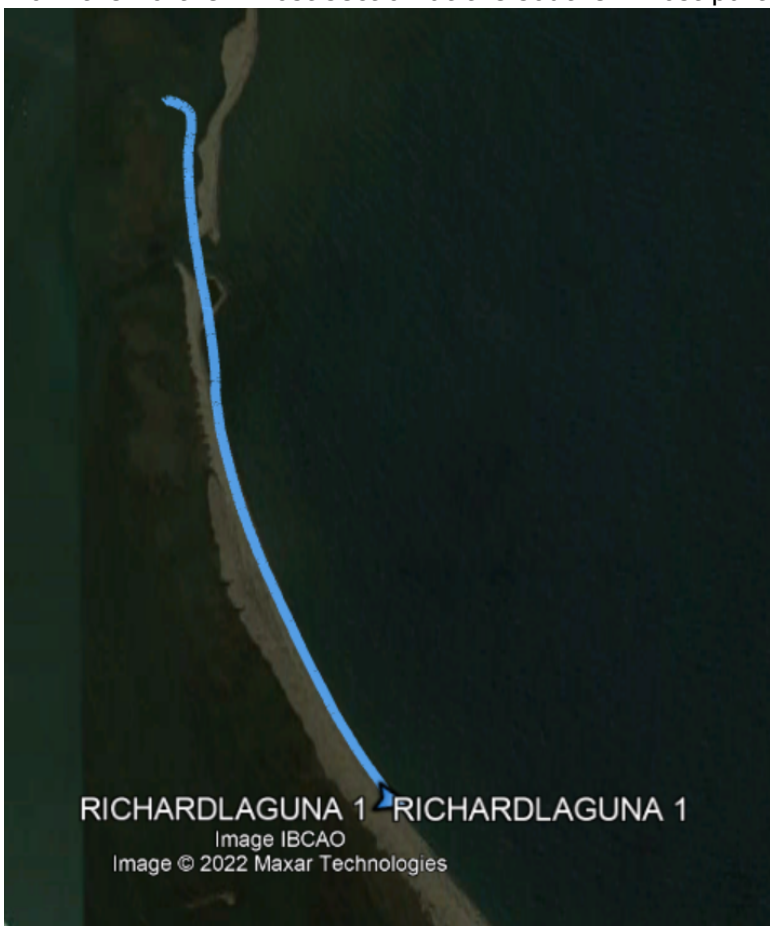

From the southernmost section at the southernmost part of Richardlaguna:

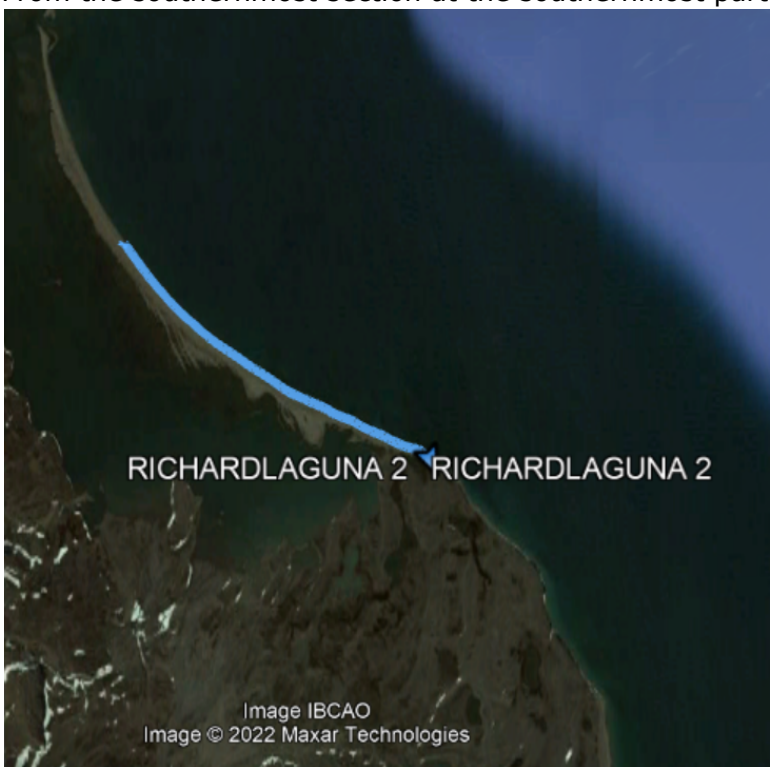

10 REFERENCES

Are, F. E. (1988). Thermal abrasion of sea coasts (part I). *Polar Geography and Geology*, *12*(1).

Atkinson, D. E. (2005). Observed storminess patterns and trends in the circum-Arctic coastal regime. *Geo-Marine Letters*, *25*(2), 98-109.

Avinash, K., Deepika, B., & Jayappa, K. (2013). Evolution of spit morphology: a case study using a remote sensing and statistical based approach. *Journal of coastal conservation*, *17*(3), 327-337.

Bader, J., Mesquita, M. D., Hodges, K. I., Keenlyside, N., Østerhus, S., & Miles, M. (2011). A review on Northern Hemisphere sea-ice, storminess and the North Atlantic Oscillation: Observations and projected changes. *Atmospheric Research*, *101*(4), 809-834.

Benedict, J. B. (1976). Frost creep and gelifluction features: a review. *Quaternary Research*, *6*(1), 55-76.

Bhattacharya, J. P. (2006). Deltas. In H. W. Posamentier & R. G. Walker (Eds.), *Facies Models Revisited.* SEPM Society for Sedimentary Geology.

Bluck, B. J. (2011). Structure of gravel beaches and their relationship to tidal range. *Sedimentology*, *58*(4), 994-1006.

Borradaile, G. (2014). Geological Maps and some Basic Terminology. In G. Borradaile (Ed.), *Understanding Geology Through Maps* (pp. 1-14). Elsevier.

Bourriquen, M., Baltzer, A., Mercier, D., Fournier, J., Perez, L., Haquin, S., Bernard, E., & Jensen, M. (2016). Coastal evolution and sedimentary mobility of Brøgger Peninsula, northwest Spitsbergen. *Polar Biology*, *39*(10), 1689-1698.

Butschek, F., Arosio, R., Austin, W. E., Noormets, R., & Howe, J. A. (2019). Late Weichselian glacial history of Forlandsundet, western Svalbard: an inter-ice-stream setting. *Arktos*, *5*(1), 1-14.

Carter, R., & Orford, J. D. (1993). The morphodynamics of coarse clastic beaches and barriers: a short-and long-term perspective. *Journal of Coastal Research*, 158-179.

Church, M., & Ryder, J. M. (1972). Paraglacial sedimentation: a consideration of fluvial processes conditioned by glaciation. *Geological Society of America Bulletin*, *83*(10), 3059-3072.

Clark, P. U., Dyke, A. S., Shakun, J. D., Carlson, A. E., Clark, J., Wohlfarth, B., Mitrovica, J. X., Hostetler, S. W., & McCabe, A. M. (2009). The Last Glacial Maximum. *Science*, *325*(5941), 710-714.

Dallmann, W. K. (2015). Historical Geology. In W. K. Dallmann (Ed.), *Geoscience Atlas of Svalbard, Rapport Series No. 148* (pp. 126-129, 291). Norsk Polaristitutt.

Dallmann, W. K. (2020). *Notes on the geology of Prins Karls Forland: review and results of geological mapping and investigations in 2012-14. Report Series No. 152*. Norsk Polarinstitutt.

Daniels, R. C. (1999). Barrier beaches and Barrier islands. In *Environmental Geology* (pp. 40-41). Springer Netherlands.

Dickson, M. E., Bristow, C. S., Hicks, D. M., Jol, H., Stapleton, J., & Todd, D. (2009). Beach volume on an eroding sand–gravel coast determined using ground penetrating radar. *Journal of Coastal Research*, *25*(5), 1149-1159.

Dingler, J. R., & Clifton, H. E. (1984). Tidal-Cycle Changes in Oscillation Ripples on the Inner Part of an Estuarine Sand Flat. *Marine Geology*, *60*(1-4), 219-233.

Eckerstorfer, M., & Christiansen, H. H. (2011). The "High Arctic maritime snow climate" in central Svalbard. *Arctic, Antarctic, and Alpine Research*, *43*(1), 11-21.

Etzelmüller, B., Schuler, T. V., Isaksen, K., Christiansen, H. H., Farbrot, H., & Benestad, R. (2011). Modeling the temperature evolution of Svalbard permafrost during the 20th and 21st century. *The Cryosphere*, *5*(1), 67-79.
Evans, O. F. (1942). The origin of spits, bars, and related structures. *The Journal of Geology*, *50*(7), 846-865.
Farnsworth, W. R., Allaart, L., Ingólfsson, Ó., Alexanderson, H., Forwick, M., Noormets, R., Retelle, M., & Schomacker, A. (2020). Holocene glacial history of Svalbard: Status, perspectives and challenges. *Earth-Science Reviews*, *208*, 103249.
Feuillet, T., Certini, G., & Ugolini, F. C. (2021). Sorted Patterned Ground. In H. Hargitai & Á. Kereszturi (Eds.), *Encyclopedia of Planetary Landforms* (pp. 1-9). Springer New York.
Fisher, R. L. (1955). Cuspate spits of St. Lawrence Island, Alaska. *The Journal of Geology*, *63*(2), 133-142.
Fjeldskaar, W., Bondevik, S., & Amantov, A. (2018). Glaciers on Svalbard survived the Holocene thermal optimum. *Quaternary Science Reviews*, *199*, 18-29.
Forbes, D. L., Orford, J. D., Carter, R. W. G., Shaw, J., & Jennings, S. C. (1995b). Morphodynamic evolution, self-organisation, and instability of coarse-clastic barriers on paraglacial coasts. *Marine Geology*, *126*(1-4), 63-85.
Forbes, D. L., Shaw, J., & Taylor, R. B. (1995a). Differential preservation of coastal structures on paraglacial shelves: Holocene deposits of southeastern Canada. *Marine Geology*, *124*(1-4), 187-201.
Forbes, D. L., & Taylor, R. B. (1994a). Ice in the shore zone and the geomorphology of cold coasts. *Progress in Physical Geography*, *18*(1), 59-89.
Førland, E. J., Benestad, R., Hanssen-Bauer, I., Haugen, J. E., & Skaugen, T. E. (2011). Temperature and Precipitation Development at Svalbard 1900–2100. *Advances in Meteorology*, *2011*, 1-14.
Forman, S., Lubinski, D., Ingólfsson, Ó., Zeeberg, J., Snyder, J., Siegert, M., & Matishov, G. (2004). A review of postglacial emergence on Svalbard, Franz Josef Land and Novaya Zemlya, northern Eurasia. *Quaternary Science Reviews*, *23*(11-13), 1391-1434.
Forman, S. L. (1990). Post-glacial relative sea-level history of northwestern Spitsbergen, Svalbard. *Geological Society of America Bulletin*, *102*(11), 1580-1590.
French, H. M. (1996). *The Periglacial Environment* (Second ed.). Harlow: Addison Wesley Longman
French, H. M. (2000). Does Lozinski's periglacial realm exist today? A discussion relevant to modern usage of the term 'periglacial'. *Permafrost and Periglacial Processes*, *11*(1), 35-42.
Friedrichs, C. T. (2011). Tidal Flat Morphodynamics: A synthesis. In E. Wolanski & D. McLusky (Eds.), *Treatise on Estuarine and Coastal Science* (Vol. 3, pp. 137-170). Elsevier.
Gallagher, C., Balme, M., Conway, S., & Grindrod, P. M. (2011). Sorted clastic stripes, lobes and associated gullies in high-latitude craters on Mars: Landforms indicative of very recent, polycyclic ground-ice thaw and liquid flows. *Icarus*, *211*(1), 458-471.
Galloway, W. E. (1975). Process framework for descrbining the morphologic and stratigraphic evolution of deltaic depositional systems. In M. L. Broussard (Ed.), *Deltas: Models for Exploration* (Second ed., pp. 87-98). Houston Geological Society. Research and Study Group.
Gao, S. (2019). Geomorphology and Sedimentology of Tidal Flats. In E. W. Gerardo Perillo, Donald Cahoon, Charles Hopkinson (Ed.), *Coastal Wetlands - An Integrated Ecosystem Approach* (Second ed., pp. 359-381). Elsevier.
Garmin. https://support.garmin.com/en-US/?faq=aZc8RezeAb9LjCDpJplTY7#:~:text=Garmin%C2%AE%20GPS%20receivers%20are,33%20feet)%20under%20normal%20conditions.
GeoSpatialExperts. Retrieved 03.03.2022 from http://www.geospatialexperts.com/ipad-gps/#:~:text=When%20you%20use%20an%20iPhone,second%20in%20latitude%20and%20longitude.

Gottschalk, J., Szidat, S., Michel, E., Mazaud, A., Salazar, G., Battaglia, M., Lippold, J., & Jaccard, S. L. (2018). Radiocarbon measurements of small-size foraminiferal samples with the Mini Carbon Dating System (MICADAS) at the University of Bern: implications for paleoclimate reconstructions. *Radiocarbon*, *60*(2), 469-491.

Hagen, J. O., Liestøl, O., Roland, E., & Jørgensen, T. (1993). Glacier Atlas of Svalbard and Jan Mayen. In A. Brekke (Ed.), *Meddelelser* (Vol. 129, pp. 12-30). Norsk Polarinstitutt.

Hanssen-Bauer, I., Førland, E. J., Hisdal, H., Mayer, S., Sandø, A. B., & Sorteberg, A. (2019). *Climate in Svalbard 2100 - A knowlege base for climate adaptation*. https://klimaservicesenter.no/kss/rapporter/klima-pa-svalbard-2100

Harris, S. A., French, H. M., Heginbotom, J. A., Johnston, G. H., Ladanyi, B., Sego, D. C., & van Everdingen, R. O. (1988a). Glossary of Terms. In S. A. Harris, H. M. French, J. A. Heginbotom, G. H. Johnston, B. Ladanyi, D. C. Sego, & R. O. van Everdingen (Eds.), *Glossary of Permafrost and Related Ground-Ice Terms* (Vol. 142, pp. 13-96). Associate Commitee on Geotechnical Research, national Research Council of Canada.

Harris, S. A., French, H. M., Heginbotom, J. A., Johnston, G. H., Ladanyi, B., Sego, D. C., & van Everdingen, R. O. (1988b). Preface. In S. A. Harris, H. M. French, J. A. Heginbotom, G. H. Johnston, B. Ladanyi, D. C. Sego, & R. O. van Everdingen (Eds.), *Glossary of Permafrost and Related Ground-Ice Terms* (Vol. 142, pp. 5-7). Associate Commitee on Geotechnical Research, National Research Council of Canada, Ottawa.

Harvey, A. M., Mather, A. E., & Stokes, M. (2005). Alluvial fans: geomorphology, sedimentology, dynamics—introduction. A review of alluvial-fan research. In A. M. Harvey, A. E. Mather, & M. Stokes (Eds.), *Alluvial Fans: Geomorphology, Sedimentology, Dynamics* (Vol. 251, pp. 1-7). Geological Society, Special Publications.

Hequette, A., & Ruz, M.-H. (1991). Spit and barrier island migration in the southeastern Canadian Beaufort Sea. *Journal of Coastal Research*, *7*(3), 677-698.

Hughes, Z. J. (2012). Tidal Channels on Tidal Flats and Marshes. In R. A. Davis & R. W. Dalrymple (Eds.), *Principles of Tidal Sedimentology* (pp. 269-300). Springer, Dordrecht.

Hume, T. M. (2005). Tidal Prism. In M. L. Schwartz (Ed.), *Encyclopedia of Coastal Science* (pp. 981-982). Springer Netherlands.

Humlum, O., Christiansen, H. H., & Juliussen, H. (2007). Avalanche-derived rock glaciers in Svalbard. *Permafrost and Periglacial Processes*, *18*(1), 75-88.

Humlum, O., Instanes, A., & Sollid, J. L. (2003). Permafrost in Svalbard: a review of research history, climatic background and engineering challenges. *Polar research*, *22*(2), 191-215.

Irrgang, A. M., Bendixen, M., Farquharson, L. M., Baranskaya, A. V., Erikson, L. H., Gibbs, A. E., Ogorodov, S. A., Overduin, P. P., Lantuit, H., & Grigoriev, M. N. (2022). Drivers, dynamics and impacts of changing Arctic coasts. *Nature Reviews Earth & Environment*, *3*(1), 39-54.

Islam, M. A., Lubbad, R., & Afzal, M. S. (2020). A Probabilistic Model of Coastal Bluff-Top Erosion in High Latitudes Due to Thermoabrasion: A Case Study from Baydaratskaya Bay in the Kara Sea. *Journal of Marine Science and Engineering*, *8*(3), 169.

Kääb, A., Girod, L., & Berthling, I. (2014). Surface kinematics of periglacial sorted circles using structure-from-motion technology. *The Cryosphere*, *8*(3), 1041-1056.

Kattsov, V. M., Källén, E., Cattle, H. P., Christensen, J., Drange, H., Hanssen-Bauer, I., Jóhannesen, T., Karol, I., Räisänen, J., & Svensson, G. (2005). Future Climate Change: Modeling and Scenarios for the Arctic. In *ACIA, 2005. Arctic Climate Impact Assessment. ACIA Overview Report* (pp. 99-144). Cambridge University Press.

Kejna, M. (2012). Introduction - 1.3 Primary Climatic Controls. In R. Przybylak, Arazny, A., Kejna, M. (Ed.), *Topoclimatic Diversity in the Forlandsundet Region (NW*

Spitsbergen) in Global Warming Conditions (pp. 17-27). Oficyna Wydawnicza "Turpress".
Kejna, M., & Araźny, A. (2012). Introduction - 1.2 Research Area and Methodology. In R. Przybylak, Arazny, A., Kejna, M. (Ed.), *Topoclimatic Diversity in the Forlandsundet Region (NW Spitsbergen) in Global Warming Conditions* (pp. 8-17). Oficyna Wydawnicza "Turpress".
Klemsdal, T. (2010). Svalbard and Jan Mayen. In E. C. F. Bird (Ed.), *Encyclopedia of the World's Coastal Landforms* (pp. 581-588). Springer Netherlands.
Kostaschuk, R., MacDonald, G., & Putnam, P. (1986). Depositional process and alluvial fan-drainage basin morphometric relationships near Banff, Alberta, Canada. *Earth Surface Processes and Landforms*, *11*(5), 471-484.
Kowalik, Z., Marchenko, A., Brazhnikov, D., & Marchenko, N. (2015). Tidal currents in the western Svalbard Fjords. *Oceanologia*, *57*(4), 318-327.
Kristensen, L., Christiansen, H. H., & Caline, F. (2008). Temperatures in coastal permafrost in the Svea area, Svalbard. Ninth International Conference on Permafrost, Fairbanks, Alaska.
Landvik, J. Y., Bondevik, S., Elverhøi, A., Fjeldskaar, W., Mangerud, J., Salvigsen, O., Siegert, M. J., Svendsen, J.-I., & Vorren, T. O. (1998). The Last Glacial Maximum of Svalbard and the Barents Sea Area: Ice Sheet Extent and Configuration. *Quaternary Science Reviews*, *17*(1-3), 43-75.
Landvik, J. Y., Ingolfsson, O., Mienert, J., Lehman, S. J., Solheim, A., Elverhøi, A., & Ottesen, D. (2005). Rethinking Late Weichselian ice-sheet dynamics in coastal NW Svalbard. *Boreas*, *34*(1), 7-24.
Lantuit, H., Overduin, P. P., Couture, N., Wetterich, S., Aré, F., Atkinson, D., Brown, J., Cherkashov, G., Drozdov, D., & Forbes, D. L. (2012). The Arctic coastal dynamics database: a new classification scheme and statistics on Arctic permafrost coastlines. *Estuaries and Coasts*, *35*(2), 383-400.
Liestøl, O. (1977). Pingos, Springs, and Permafrost in Spitsbergen. In A. Brekke, T. S. Winsnes, P. Hagevold, V. Hisdal, & T. Larsen (Eds.), *Årbok 1975* (pp. 7-29). Norsk Polarinstitutt.
Lutgens, F. K., Tarbuck, E. J., & Tasa, D. (2014a). Shorelines. In F. K. Lutgens, E. J. Tarbuck, & D. Tasa (Eds.), *Essentials of Geology* (Vol. 11, pp. 343-372). Pearson Prentice Hall.
Lutgens, F. K., Tarbuck, E. J., & Tasa, D. (2014b). Weathering and Soils. In F. K. Lutgens, E. J. Tarbuck, & D. Tasa (Eds.), *Essentials of Geology* (Vol. 11, pp. 143-170). Pearson Prentice Hall.
Masselink, G., Hughes, M. G., & Knight, J. (2011a). Coasts and Climate. In G. Masselink, M. G. Hughes, & J. Knight (Eds.), *Introduction to Coastal Processes and Geomorphology* (2 ed., pp. 349-371). Hodder Education.
Masselink, G., Hughes, M. G., & Knight, J. (2011b). Fluvial-Dominated Coastal Environments - Deltas. In G. Masselink, M. G. Hughes, & J. Knight (Eds.), *Introduction to Coastal Processes and Geomorphology* (2 ed., pp. 148-177). Hodder Education.
Masselink, G., Hughes, M. G., & Knight, J. (2011c). Wave-Dominated Coastal Environments - The Shoreface, Beaches and Barriers. In G. Masselink, M. G. Hughes, & J. Knight (Eds.), *Introduction to Coastal Processes and Geomorphology* (2 ed., pp. 211-266). Hodder Education.
Mather, A. E., & Stokes, M. (2018). Bedrock structural control on catchment-scale connectivity and alluvial fan processes, High Atlas Mountains, Morocco. In D. Ventra & L. E. Clarke (Eds.), *Geology and Geomorphology of Alluvial and Fluvial Fans: Terrestrial and Planetary Perspectives* (Vol. 440, pp. 103-128). Geological Society, Special Publications.
Mayhew, S. (2009). *A Dictionary of Geography*. Oxford University Press. https://doi.org/10.1093/acref/9780199231805.001.0001
McColl, S. T. (2012). Paraglacial rock-slope stability. *Geomorphology*, *153*, 1-16.
Missana, A. F. J. M. (2021). *Mapping and dating Holocene advances of Nansenbreen on Erdmannflya, Svalbard* MSc, University Centre in Svalbard, Longyearbyen.

Mulhern, J. S., Johnson, C. L., & Martin, J. M. (2017). Is barrier island morphology a function of tidal and wave regime? *Marine Geology*, *387*, 74-84.
Mulhern, J. S., Johnson, C. L., & Martin, J. M. (2019). Modern to ancient barrier island dimensional comparisons: implications for analog selection and paleomorphodynamics. *Frontiers in Earth Science*, *7*, 109.
Norðdahl, H., & Ingólfsson, Ó. (2015). Collapse of the Icelandic ice sheet controlled by sea-level rise? *Arktos*, *1*(1), 1-18.
NPI, N. P. I. Retrieved 10.10.2021 from https://geokart.npolar.no/Html5Viewer/index.html?viewer=Svalbardkartet
NPI, N. P. I. Retrieved 27.09.2021 from https://toposvalbard.npolar.no/
NRK. (2022). *Her stig ikkje havet, her er det landet som hevar seg*. Retrieved 15.05.2022 from
Oertel, G. F. (1985). The barrier island system. In (Vol. 63, pp. 1-18): Elsevier.
Orford, J. D., Carter, R. W. G., & Forbes, D. L. (1991b). Gravel Barrier Migration and Sea Level Rise: Some Observations from Story Head, Nova Scotia, Canada. *Journal of Coastal Research*, *7*(2), 477-489.
Orford, J. D., Carter, R. W. G., & Jennings, S. C. (1991a). Coarse Clastic Barrier Environments: Evolution and Implications for Quaternary Sea Level Interpretation. *Quaternary International*, *9*, 87-104.
Otvos, E. G. (2012). Coastal barriers—Nomenclature, processes, and classification issues. *Geomorphology*, *139*, 39-52.
Parry, S. (2011). The application of geomorphological mapping in the assessment of landslide hazard in Hong Kong. In *Developments in Earth Surface Processes* (Vol. 15, pp. 413-441). Elsevier.
Reading, H. G., & Collinson, J. D. (1996). Clastic Coasts. In H. G. Reading (Ed.), *Sedimentary Environments: Processes, Facies and Stratigraphy* (Third ed., pp. 154-232, 688). Blackwell Science.
Reineck, H.-E., & Singh, I. B. (1980). Tidal flats. In *Depositional sedimentary environments* (pp. 430-456). Springer.
Salvigsen, O. (1976). Radiocarbon datings and the extension of the Weichselian ice-sheet in Svalbard. In A. Brekke (Ed.), *Årbok* (Vol. 1976, pp. 209-224). Norsk Polarinstitutt.
Savelieva, N., Semiletov, I., Vasilevskaya, L., & Pugach, S. (2000). A climate shift in seasonal values of meteorological and hydrological parameters for Northeastern Asia. *Progress in Oceanography*, *47*(2-4), 279-297.
Serreze, M., Box, J., Barry, R., & Walsh, J. (1993). Characteristics of Arctic synoptic activity, 1952–1989. *Meteorology and Atmospheric Physics*, *51*(3), 147-164.
Serreze, M. C., Holland, M. M., & Stroeve, J. (2007). Perspectives on the Arctic's shrinking sea-ice cover. *Science*, *315*(5818), 1533-1536.
Shur, Y., & Osterkamp, T. E. (2007). *Thermokarst* (INE06.11). U. o. A. F. Insitution of Northern Engineering.
Simmonds, I., & Keay, K. (2009). Extraordinary September Arctic sea ice reductions and their relationships with storm behavior over 1979–2008. *Geophysical Research Letters*, *36*(19).
Skinner, L. R. (2022). *MSc in preparation: Quantification of Svalbard´s Coastline since 1936* MSc i preparation, University Centre in Svalbard, Longyearbyen.
Smedsrud, L. H., Muilwijk, M., Brakstad, A., Madonna, E., Lauvset, S. K., Spensberger, C., Born, A., Eldevik, T., Drange, H., & Jeansson, E. (2022). Nordic Seas heat loss, Atlantic inflow, and Arctic sea ice cover over the last century. *Reviews of Geophysics*, *60*(1), e2020RG000725.
Sobota, I., & Nowak, M. (2014). Changes in the Dynamics and Thermal Regime of the Permafrost and Active Layer of the High Arctic Coastal Area in North-West Spitsbergen, Svalbard. *Geografiska Annaler: Series A, Physical Geography*, *96*(2), 227-240.
Sollid, J. L., & Christiansen, H. H. (2003). *Permafrost, periglacial features and glaciers in Svalbard, Excursion Guide. VIII* (Vol. 14). Geografisk Institutt, Universitet i Oslo.

Stéphan, P., Suanez, S., Fichaut, B., Autret, R., Blaise, E., Houron, J., Ammann, J., & Grandjean, P. (2018). Monitoring the medium-term retreat of a gravel spit barrier and management strategies, Sillon de Talbert (North Brittany, France). *Ocean & Coastal Management*, *158*, 64-82.

Svendsen, H., Beszczynska-Møller, A., Hagen, J. O., Lefauconnier, B., Tverberg, V., Gerland, S., Børre Ørbæk, J., Bischof, K., Papucci, C., & Zajaczkowski, M. (2002). The physical environment of Kongsfjorden–Krossfjorden, an Arctic fjord system in Svalbard. *Polar research*, *21*(1), 133-166.

Svendsen, J. I., & Mangerud, J. (1997). Holocene glacial and climatic variations on Spitsbergen, Svalbard. *The Holocene*, *7*(1), 45-57.

Tribe, H. M., & Kennedy, D. M. (2010). The geomorphology and evolution of a large barrier spit: Farewell Spit, New Zealand. *Earth Surface Processes and Landforms*, *35*(15), 1751-1762.

Van Rijn, L. C. (2013). *Erosion of gravel/shingle beaches and barriers* EU-Project CONSCIENCE, https://www.leovanrijn-sediment.com/papers/Gravelbeaches2013.pdf

Walczowski, W., & Piechura, J. (2011). Influence of the West Spitsbergen Current on the local climate. *International journal of climatology*, *31*(7), 1088-1093.

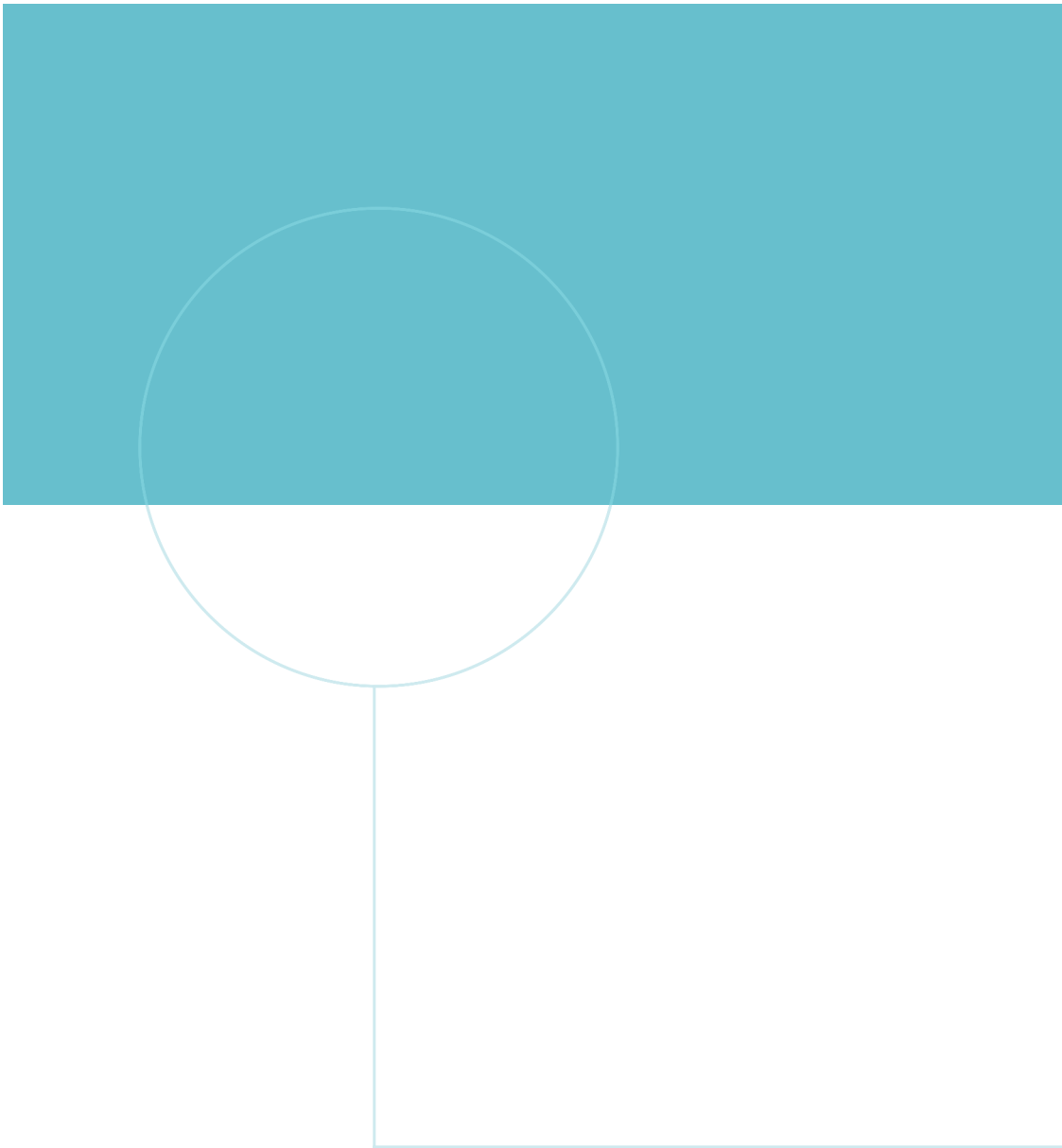

NTNU

Kunnskap for en bedre verden